Republic of Iraq
Ministry of Higher Education & Scientific Research
University of Baghdad
College of Education for Pure Sciences Ibn Al-Haitham
Department of Physics

Calculating and Analysing of Some Atmospheric Effects on the Beam of Free Electron Laser

A thesis Submitted

To

The council of College of Education for pure science/Ibn Al-Haitham, University of Baghdad in Partial Fulfillment of the Requirements for the Degree of Master of Science in Physics

By

Rasheed Lateef Jawad

B.Sc. In Physics Sciences 2014

Supervisor

*Asst. Prof. Dr. **Thair Abdulkareem Khalil Al-Aish***

2017 A.D.   *1438 A.H.*

بِسْمِ ٱللَّهِ ٱلرَّحْمَٰنِ ٱلرَّحِيمِ

قَالُوا۟ سُبْحَٰنَكَ لَا عِلْمَ لَنَآ إِلَّا مَا عَلَّمْتَنَآ إِنَّكَ أَنتَ ٱلْعَلِيمُ ٱلْحَكِيمُ

صدق الله العلي العظيم

﴿٣٢﴾ سورة البقرة

Supervisors Certification

We certify that Rasheed Lateef Jawad has presented this thesis under our supervision at physics department, College of Education for Pure Sciences Ibn- AL-Haitham, the University of Baghdad as a partial requirement for the degree of Master of Science in physics.

Signature:

Name: **Dr. Thair Abdulkareem Khalil Al Aish**

Title: Assist Professor

Address: College of Education for Pure Science Ibn Al-Haitham

University of Baghdad

Date: 8 / 1 / 2018

In view of the available recommendation, I forward this thesis for debate by the examination committee.

Signature:

Name: **Dr. Kareem Ali Jasim**

Title: Professor

Address: College of Education for Pure Science Ibn Al-Haitham

University of Baghdad

Date: / / 2018

Certification of Examiners

We certify, that we have read the thesis titled *"Calculating and Analysing of Some Atmospheric Effects on the Beam of Free Electron Laser"*, presented by *Rasheed Lateef Jawad* and as an examining committee, we examined the student on its contents, and in what is related to it, and that in our opinion it meets the standard of a thesis for the degree of Master of Science in Physics Science.

(Chairman)

Signature:

Name: *Dr. Alaa Badr Hasan*
Title: *Assistant Professor*
Address: *University of Baghdad*
Date : 3 / 1 / 2018

(Member)

Signature:

Name: **Dr. Tareq Hashim Abbood**
Title: *Assistant Professor*
Address: *AL-Mustansiriyah University*
Date : 3 / 1 / 2018

(Member)

Signature:

Name: **Dr. Ebtisam Mohammed Taki**
Title: *Lecturer*
Address: *University of Baghdad*
Date : 3 / 1 / 2018

(Supervisor)

Signature:

Name: **Dr. Thair Abdulkareem Khalil Al Aish**
Title: *Assistant Professor*
Address: *University of Baghdad*
Date: 3 / 1 / 2018

Approved by the Dean of College of Education for Pure Science (Ibn Al- Haitham)/ University of Bagdad

(The Dean)
Signature:
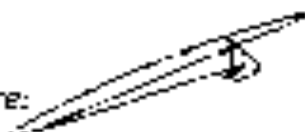Name: *Dr. Khalid Fahad Ali*
Title: *Professor*
Date: / / 2018

Linguistic Amendment

I certify that this thesis titled "*Calculating and Analysing of Some Atmospheric Effects on the Beam of Free Electron Laser*" presented by (*Rasheed Lateef Jawad*) has been corrected linguistically; therefore, it is suitable for debate by the examining committee.

Signature:

Name: **Haitham Akram**

Date: 9 / 1 / 2018

To my family,

who offered me unconditional support

throughout the course of this thesis

To my Teachers,

who provided me the keys of success

Rasheed

Acknowledgements

Praise is to Allah, peace is to be upon Prophet Mohammed and his relatives and companions.

First, I would like to thank my supervisor, Dr. Thair Abdulkareem Khalil Al-Aish, for the countless hours that he dedicated to this thesis. His understanding and expertise in my area of research greatly improved the contents of this thesis. I am grateful for his helpful comments, suggestions and constructive criticism throughout this project. I have got benefit substantially from his insightful recommendations. Dr. Thair was and still as close as a brother and a good friend to me.

I would like to express my thanks to the staff of Physics Department in College of Education for Pure Sciences Ibn Al-Haitham in Baghdad University for their help.

Last but not least, thanks for my friends and my colleagues who supported me a lot during the two years of study and were of great help.

.

Rasheed

Abstract

In this work, a new model is designed of free electron laser defenses system FELDS in infrared range with high output power to destroy any target (missile, aircraft) at range 70 Km of sea level. The design of any defense system requires knowledge of the characteristics of the target that will be destroyed, the range of the target and its movement whether directed towards of the defense system or away from it.

The design of free electron laser FEL oscillator includes four basic ingredients an electrons gun, electrons accelerator, a static periodic magnetic-field (undulator) and an optical resonator.

In order to simulate the defense system, and determine the parameters of that system, it has been established a special program using the language visual basic software 2010, which contains many parameters to calculate and analyze the atmospheric effect (such as absorption, scattering, fog, rain, reflection index, refraction index and beam diverges) on the laser beam of FELDS when passes through the different atmospheric layers.

Table of Contents

Chapter Three: Design and Simulate of Free Electron Laser Defenses System FELDS

Chapter four: Results & Discussion

Chapter Five: Conclusions & Suggestions for Future Work

APPENDIX   65
References

List of Tables

List of Figures

List of Symbols

Symbol	Meaning	Unit
λ	Laser wavelength	A^0
γ	Relativistic lorentz-factor	/
K	Wiggler parameter	/
λ_m	Wavelength of wiggler	cm
B_w	Magnetic field of wiggler	Tesla
m_e	Electron mass	kg
c	Speed of light	m/sec
N_u	Number of undulator periods	/
E_{beam}	Electron beam energy	MeV
P_z	Laser power out from wiggler	kW
Z_w	Undulator length	m
N_{PH}	Number of coherent photons per electron	/
P_{sat}	Power after passing a distance (Z_w) through the wiggler	GW
L_G	Gain length	m
E_{Ph}	Photon energy	eV
χ	Scaling parameter of FEL	/
a_w	The dimensionless vector potential of the wiggler	/
w_p	Plasma frequency of the beam	Hz
$F(k)$	Undulator-radiation coupling factor	/
J_0, J_1	Bessel functions	/
w_c	The central-frequency of the emitted radiation	Hz
n_e	Electron beam density	m^{-3}
I_{beam}	Beam current	kA

e	Electron charge	C
r_e	The classical radius of the electron	m
P_0	The initial power	W
P_{beam}	Electron beam power	MW
g_w	Undulator gap	mm
Q	Electron beam charge	C
$\sigma'_{x,y}$	Electron beam divergence	mrad
σ_x	The electron beam sizes in x directions	μm
σ_y	The electron beam sizes in y directions	μm
ε_x	Normalized emittance in the x directions	μm
ε_y	Normalized emittance in the y directions	μm
σ_δ	Energy spread of electron beam	/
R_1, R_2	Reflection of mirrors	/
L_c	Distance between two mirrors	m
r_1	The radius of curvature of a first mirror	m
r_2	The radius of curvature of a second mirror	m
g_1, g_2	Parameters resonator stability	/
P_m	Free electron laser defense system FELDS power	kW
G	laser gain parameter	m⁻¹
$\forall$	Laser losing parameter	m⁻¹
$I_{(r,z)}$	Distribution of irradiance	W/m²
I_0	The irradiance at the center of the beam central	W/m²
r	The radial-distance from the optical axis	mm
Z_R	The Rayleigh-length	m
ω_0	Waist radius of the laser	mm

A_{beam}	The beam cross-section	mm^2
$d_{(mirror)}$	Beam spot size that out from mirror	mm
d_0	The diameter of beam waist	mm
M^2	The quality-factor	/
T_A	Temperature degree	K
P_A	Pressure	mbar
ρ_A	Density	kg/m^3
T_{base}	The temperature at the base of the layer	K
L_{rate}	The change in temperature rate	K/km
R_r	The range of target	km
R_A	The altitude	km
R_{base}	The altitude at the base of the layer	km
P_{base}	The pressure at the base of the layer	mbar
r_{gas}	The real gas constant for air	$m^2/K.sec^2$
g	The acceleration of gravity	m/sec^2
β_{Sc}	Scattering coefficient	1/km
β_{Sn}	Snow attenuation coefficient	1/km
S	The snow rate	mm/hour
a,b	The value of the parameter of dry and wet snow	/
β_{ra}	The rain attenuation coefficient	1/km
R_{ra}	The rainfall rate	1/km
P_{Ds}	Laser power on target	kW
β	The total attenuation	1/km
n	The refractive index of air	/
C_n^2	Index refraction structure factor	$m^{-\frac{2}{3}}$

r_i	A scalar distance between areas	m
r_0	The Fried parameter	m
D_{ta}	The distance that target will move	cm
v_{ta}	The speed of the target	m/sec
δ	Laser beam divergence	m
Γ	The intensity on the target	W/cm²
P_{Tm}	The power needed for destroying the target	kW
A	The cross sectional area of the beam spot on the target	cm²
F	The total energy delivered per unit area	J/cm²
t_{in}	Time the laser is on the target (dwell time)	sec
ω_r	The laser beam spot radius.	cm³
E_t	The total energy required to apply on target	J
ρ_m	Density of material	g/cm³
d_t	Thickness of the material	mm
C	Target specific heat capacity	J/gm.C⁰
T_m	Melting-point of target material	C⁰
T_R	Temperature of the target at altitude R_A	K
L_m	Latent heat of melting of target surface	J/gm
T_v	Target vaporizing point	C⁰
L_v	Latent heat of vaporizing of target surface	J/gm
P_{actual}	The actual power needed to be applied to the target	kW

List of abbreviations

Abbreviation	Meaning
FEL	Free electron laser
DE	Directed Energy
DEWs	Directed energy weapons
HPM	High Powered Microwaves
Sm-Co	Samarium-Cobalt magnets
PPM	Pure Permanent magnetic
LPA	Laser Plasma Accelerator
SIOM	City in China
FELDS	Free electron laser defenses system

Chapter One
Introduction and
Literature Survey

Chapter one

Introduction and Literature Survey

1.1 Introduction

The laser is one of the top technological achievements of the 20th century, which has become increasingly affecting applications in various fields of civil and military life. It is a coherent beam with a wavelength that covers a wide range of electromagnetic spectrum in the confined area between infrared (around $10^5 \ A^0$) and ultraviolet radiation (around $2000 \ A^0$) [1].

It should be noted, that most conventional laser types are not readily available within the far infrared region of the spectrum (around $3x10^5 \ A^0$ to $10^7 \ A^0$), or at X-ray wavelength (less than $100 \ A^0$). Therefore, there is a suitable alternative laser covering these two areas in the electromagnetic spectrum, this type is called the free electron laser (FEL) [2].

FEL uses a beam of electrons passing through a periodic, transverse magnetic field to produce coherent radiation. Source of these electrons is an electron accelerator, like a linear accelerator (linac) or a synchrotron. The undulator (sometimes called "Wiggler") is a magnetic device to produce a static magnetic field, which transforms part of the kinetic energy of electrons into coherent electromagnetic radiation. The FEL has many important advantages compared to conventional laser such as [2-4]:

1. **Wide Tunability** : The production of FEL can be controlled to become a wavelength beam in any region of the electromagnetic spectrum by varying

either the Intensity of magnetic field (B_m) or the electron beam energy (E_{beam}).

2. **Short Pulses:** It is known that ultra-short pulses cannot be produced at all wavelengths in conventional lasers. But the FEL can obtain ultra-short pulses at all wavelengths because the structure of the radiation pulse simulates that of the electron pulse.

3. **High Brightness**: The FEL can produce with high brightness in both regions IR and X-ray. In IR, the FEL can provide brightness that is three to four orders of magnitude higher than synchrotron radiation sources or conventional laboratory sources [5].

4. **Short-Wavelength:** In the FEL can be generating high power, short pulse and short wavelengths in term short X-ray.

5. **High Power:** The high power in conventional laser has disadvantages such as heating and breakdown of the laser medium. But in the free electron laser principle there is no fundamental limit because the electron beam (laser medium) exits the interaction volume at close to the speed of light, and electrons cannot breakdown.

1.2 Directed High-Energy Laser

The technologies of Directed-Energy (DE) encompass a vast field of non-kinetic capabilities that generate beams or fields of electromagnetic energy. Directed energy weapons (DEWs) propagate this energy to engage a target remotely at the speed of light [6,7].

One of the main benefits of Directed Energy technologies is scalability effects on the target, this effect that ranges from temporary-disruption to permanent damage. With High-Powered-Microwaves (HPM) effects can range

from interruption (shutting off an engine) to permanent damage to electronics within the target. The advantages of using High-Energy laser defense system are: [8,9]

1. The laser beams travel at the speed of light. This leads to reach the target during parts of the second.

2. The ammunition limitless in laser weapon system.

3. The laser weapon system can destroy the target with any range by controlling out-power.

4. There is no collateral damage when using laser weapon to the environment like bombings or chemical radiation.

5. It's very easy to control the direction of the laser beam by using the mirror and focusing it on target.

6. The cost is very low, which makes the laser weapon system effective compared with conventional weapons.

While the disadvantages of using High-Energy laser defense system are [10]:

1. The High-Energy laser defense system needed to the high amount for electrical power.

2. The laser beam suffers from losing the power when traveling in the air occurs by the atmosphere effect.

3. The high size of the laser weapon makes it fixed targets and it is easy to destroy.

4. The turbulence of the atmospheric layer lead to change in the refractive index and this leads to change in the direction of the laser beam when it propagation through different atmospheric layers.

5. High reflectivity of the target surface (aluminum or steel) which leads to a high loss of laser beam energy when the laser beam falls on the target

1.3 The Atmospheric Effects

The atmosphere of earth effects on the propagation of laser beam, where these effects happen at different points in the atmosphere. The atmosphere of earth can be classified into the following regions [11,12]:

1. Troposphere: Stretch from the surface of the earth between (0-11 km) above the earth's surface, the turbulence abounds in this region are due to a lot of thermal movement of air. The temperature of air decreases strongly as altitude increases due to expensive cooling.
2. Stratosphere: Starts from the end of the troposphere and ends at the altitude (50 km). In this layer it can be found ozone layer.
3. Mesosphere: Stretch from (50 to 80-85 km) above the Earth's surface.
4. Thermosphere: Starts from the end of the mesosphere and ends at the altitude (+640 km) this layer contains the ionosphere which is a region of highly charged particles due from the ionization of atmosphere atoms molecules from solar radiation.
5. Exosphere: This layer stretch to approximately 10,000 km.

The most important effects of atmospheric on the laser beam propagation are (refraction, reflection, scattering, absorption, rainfall and snowfall). These effects occur in the Tropospheric layer because the refractive-index of the atmosphere decreases with the increase of the altitude, leading to a bending of waves back toward the earth. All these phenomena are presented in Chapter Two.

1.4 Literature Survey

The following review briefly shows the results of some previous researchers on free electron laser and atmospheric effects on the laser beam.

In **1971 J. M. MADEY**, was able to calculate the gain achieved in the movement of the relative electron while passing through a periodic magnetic field using Weizsacker-Williams method [13].

In **1976 L. R. Elias and others,** Studied the gain of the optical radiation at 1.06×10^5 A^0, a gain of 7% per pass was obtained at an electron current of 70 mA, and found the gain of for optical radiation at 1.06×10^5 A^0 [14].

In **1980 R. Ruquist**, studied the variable atmosphere effects on high energy laser propagation, where they developed a method to determine the propagation performance based on an annual probability. They developed a statistical model of thermal blooming, a nonlinear absorption phenomenon which limits the spread of the laser beam[15].

In **1984 R. Bonifacio and C. Pellegrini**, studied the high gain of free electron laser and the development of a study of its behavior. In addition to setting special conditions for the emergence of a collective instability in the electron beam undulator field system and set the criteria for obtaining the best way to produce the greatest radiation energy[16].

In **1988 K. S. Shaik**, studied the optical communication and the factors that affect it, such as clear-air turbulence and atmospheric turbidity, beam broadening, the angle of arrival, absorption and scattering and the effect of opaque clouds [17].

In **1996 E. J. Anderson**, explained the possibility of integrating a 1 MW infrared FEL with ship systems perspective and studied the factors affecting on the effectiveness of this system [18].

In **1997 S. Zhengfang,** studied and analyzed the effect of a number of atmospheric attenuation such as absorption, reflectivity and scattering on laser beam transmission of different types of laser (GaAs, YAG, HF, DF, and CO_2), and found that the CO_2 laser is suitable for adverse weather conditions within a range of 5 km, as well the DF laser is superior to all other lasers in propagation property, and is slightly inferior to the HF laser only at an emission altitude more than 10 km. [19].

In **2001 N. Ivan**, studied the possibility of using the free electron laser as a weapon, and shows the effect of atmospheric attenuation (thermal blooming, and turbulence) on the laser beam power (1.5 MW), and also the number of targets that can be destroyed by this weapon [20].

In **the same year I. I. Kim and others**, , studied the optical wireless communications and propagation of laser beam at 7850 A^0 and 15500 A^0 in fog and haze, it was found that in hazy weather (visibility > 2 km), the prediction of less atmospheric attenuation at 15500 A^0 is most likely true.in foggy weather (visibility < 0.5 km), and the attenuation of laser light is independent of wavelength 7850 A^0, 8500 A^0, and 15500 A^0 are all attenuated equally by fog. this same wavelength independence is also observed in snow and rain [21].

In **2002 G. Dattoli and P. L. Ottaviani**, Enables a detailed description of the free electron laser (especially linear regime and saturation) and put new

semi-analytical models of higher order Super Modes dynamics, high gain and harmonic generation mechanisms [22].

In **the same year X. Yaoheng and F. Hesheng**, analyzed the range of the laser beam during its propagation in the atmosphere (Gaussian distribution), and explained the effect of atmospheric turbulence on it, in addition to the conclusion of a new form of the equation for the spread of laser beam [23].

In **the same year S. Krinsky**, Explained basic principles for the operation of a free electron laser, and how to optimize the amplification process to get the best possible gain and the best performance [24].

In **2006 C. Pellegrini**, Enables the generation of free electron laser with wavelengths ranging between nanometer and short nanometer, and review the theoretical and experimental status of X-ray and Soft X-ray FELs [25].

In **the same year D. COWAN**, studied the effects of atmospheric turbulence on the propagation of flattened Gaussian optical beams, and explained the effective spot size of the flattened beam at the transmitter, then found and developed the first and second order moments of the Rytov approximation. That led to the conclusion an analytical expression for the scintillation index [26].

In **2007 Z. Huang and K. Kim**, studied the basic theory of the free electron lasers (FELs), and they explained a number of basic processes such as self-amplified spontaneous emission, the saturation of the high-gain, transverse coherence, temporal characteristics and harmonic content [27].

In **2008 M. Beshr and M. H. Aly**, studied the effect of visibility range on the atmospheric attenuation of the outdoor wireless optical communication system. Then, they explained the wavelengths effect (7800, 13×10^3 and 155×10^2 A^0)on the atmospheric attenuation is also investigated [28].

In **2009 M. A. Hussein**, A detailed study of satellite communication was conducted, and explained a number of fundamental processes affecting the spread of the beam during the atmosphere, such as attenuation caused by tropospheric scintillation, meteorological conditions, frequency, antenna diameter and elevation angle on the magnitude of scintillation and it was a prediction method suggested to measure tropospheric scintillation on the earth-space path [29].

In **the same year L. Dordov´a and O. Wilfert**, had a detailed study of optical signal(media) attenuation which was conducted, and a number of basic operations were shown during the spread of the beam through atmosphere layers such as optical intensity distribution, atmospheric turbulence, Rytov approximation and found that the turbulent atmospheric transmission medium using the 15500 A^0 wavelength is less attenuated than 8500 A^0 wavelength [30, 31].

In **2012 M. A. Abd Ali**, made a detailed study of attenuation for different wavelengths (Free Space Optics) under different weather attenuating conditions (fog, rain and snow). it was found that the optimum wavelength is 155×10^5 A^0 and provides a significant improvement in the performance as compared to other wavelengths [32].

In **the same year A. Alkholidi and K. Altowij**, a detailed study of free space optics attenuation for different wavelengths (7800 A^0, 8500 A^0 and 15500

A^0) under different weather attenuating conditions (fog, rain and snow) , and explained a number of fundamental parameters affecting on the spread of the beam during the atmosphere, such as scattering coefficient, atmospheric attenuation، beam divergence angle, absorption, transmitter and receiver diameter apertures and transmission range .It has been explained that the scattering occurs when the size of the molecule is less than the laser beam wavelength [33].

In **the same year M. Bakr and others**, reviewed a design and numerical simulation of Terahertz FEL amplifier, the system was consisting of 1.6 cell photocathode radio frequency (RF) gun to get wavelength with the range about $15x10^5\ A^0 - 34x10^5\ A^0$, THz-wave parametric generator, focusing solenoid, transport line and 1.2 m long undulator with 30 periods. it was found that 1250% amplification could be achieved in the resonance of present design [34].

In **2013 M. A. Abd Ali and M. A. Mohammed**, made a detailed study of the optical signal in free space (FSO), and explained a number of weather parameters affecting on the spread of optical signal with ranges (6500, 7850 and 15500) A^0, such as attenuation coefficient, receiver optical power, data transfer rate and link margin under the influence of the weather conditions, found that weather conditions such as (clear, haze, thin fog, light fog and heavy fog) effect on those wavelengths at different ways. Where it was able to improve performance by increasing the transmitted power and reduce the divergence angle of the laser beam [35].

In **the same year P. Pan**, made a detailed study of the turbulence theory by using the measurement of the scintillation index and the angle-of-arrival fluctuation, he was able to find the most influential factors in the turbulence,

namely the refractive index fluctuations C_n^2 and the inner scale of the turbulence [36].

In **the same year M. A. Shanshoul and others**, made a detailed study of atmospheric penetration factors for near infrared laser beam (9800 A^0) performing as a carrier data in free space rainy atmospheric conditions, found that the outcomes have shown the importance of both condensed water as a factor with the main effect on the atmosphere attenuation which results from absorption and the aerosol and rain as factors with an effect on the laser beam attenuation according to the scattering concept [37].

In **the same year A. R. Jabbar and Others**, studied the effect of the attenuation of the fog on the transmitted laser power and transmitter range (propagation distance) where they took five different values of transmitted laser power, They are (50 mW, 40 mW, 30 mW, 20 mW, 10mW) and calculate the maximum send range of each value of the values of the power transmitted under the effect of Fog attenuation of wavelength (15500 A^0, 7840 A^0), they found that the attenuation fog increases, the less visibility, and the attenuation of fog when the wavelength (15500 A^0) is less than the attenuation fog when the wavelength (7840 A^0), as well they found that attenuation Fog effects on the transmitted laser power through the atmosphere and thus will affect the range of the transmitter and the performance of the system in general [38].

In **2014 M. A. Ali**, studied the turbulence attenuation and their effect on optical beam in free space and analysis the atmospheric turbulence effect between two classical methods, Rytov approximation and Andrews's method and used the range of wavelengths 8500 A^0 and 15500 A^0 and the distance between the

transmitter and receiver horizontal link set to value range (0 km -2 km), it was found that the wavelength 15500 A^0 has the best signal to noise ratio compared with the wavelength 8500 A^0 at the same strength of turbulence α and refractive index structure parameter C_n^2 [39].

In **the same year L. Song and others**, made a detailed study of the common factors affecting on the laser propagation in the atmosphere under complex weather conditions. It was found that the optimum , from simulation results found that in haze days the bit error rate (BER) renders linear change with the visibility and the dry snow has the greatest impact on the bit error rate in haze days the bit error rate is sensitive to the zenith angle, in moderate rainy days the bit error rate has an approximately linear correlation with the zenith angle, and the impact of heavy fog and moderate snow on zenith angle is very small [40].

In **the same year A. N. Rashed and M. S. Tabbour**, made a new study of the free space optics and submarine laser communications was conducted, and explained a number of fundamental processes affecting the spread of the beam during the atmosphere, such as optical path length, optical intensity fluctuations, the coefficient of Rayleigh scattering, temperature, wind speed, signal altitude over ground, and relative humidity variations. It was explained, increasing the signal to noise ratio and decreasing bit error rate and laser intensity, arrival angle fluctuations. Where the signal to noise ratio changed when increasing optical link range, increased both bit error rate and laser intensity and angle of arrival fluctuations, and observed that the increased operating optical laser wavelength [41].

In **2015 M. Firoozmand and M. Naser,** studied the modeling and simulation of fading due of atmospheric turbulence that effect on the laser beam

like absorption, scattering, and turbulence this phenomenon will give rise to disorder on the amplitude, wavelength, and phase of the wave. The wave-front deviation and phase deviation are results of the atmospheric turbulence that causes fading of the beam from receiver aperture. The refractive-index incoherence (between transmitter and receiver) due to the atmosphere interplay, is the cause of turbulence, it was found that from the simulation that eddy sizes are more than 0.1 km for weak turbulence and with increase C_n^2 (The parameter of refractive-index structure) the eddy sizes will have decreased. Increased C_n^2 will have caused increased variance of refractive index [42].

In **the same year S. D. Mitri**, proposed review which illustrates a new to the design of free electron laser, and analyze the relation between the output wavelength, exponential gain length, and electron beam brightness, it was extending the discussion to include the three dimensional effects of FEL and electron beam projected emittances [43].

In **2016 S. A. Kadhim and Others**, studied the spectrum attenuation of free space optical communication systems operating at visible and near-infrared wavelengths (6500 A^0 and 8500 A^0) under fog and smoke, it was found that the selection of higher wavelength range for moderate to the dense fog conditions where V < 0.5 km, is not a suitable solution in order to mitigate the fog attenuation for free space optical communications [44].

In **2017 R. Bonifacio and others**, proposed a new design of sub-angstrom compact FLE source, it was used a Compton backscattering scheme to build the design to obtain very high beam quality [45].

In **the same year T. Liu and Others**, proposed a new design to maintain the superior features of the LPA beam and a transverse gradient undulator (TGU). it was using a compact scheme of the LPA beam to achieve high gain at a wavelength of 300 A^0.It was explained the effect of strong focusing quadruples, the chromatic correction on the laser beam [46].

1.5 Aim of this Project

1. Design a new model of free electron laser defenses system FELDS in infrared range with high out power to destroy any target (missile, aircraft) at range 70 Km of sea level.

2. Calculation and analysis of the atmospheric effect (such as absorption, scattering, fog, rain, reflection index and beam diverges) on the laser beam.

1.6 Outline of the thesis

The thesis is organized according to the following scheme. The current chapter (Chapter one) provides a brief introduction to the research topic and a statement of the motivations and objectives of the research and provides a survey of the literature of free electron laser and the effect of the atmosphere on the laser beam. Chapter two provides a theoretical framework of the research area. Chapter three includes a design of free electron laser defense system (FELDS) and calculating that affect parameter on the FELDS. The results and discussion are presented in chapter four. Chapter five contains the conclusions of calculating and Analysis of Atmospheric Effects on the Beam of High-Energy Laser, as well as recommendations for future works.

CHAPTER TWO

THEORETICAL BACKGROUND

CHAPTER TWO

THEORETICAL BACKGROUND

2.1 Free Electron Laser Theory

2.1.1 Introduction

At present, the laser is an essential application in various civilian and military fields. Where, it is used in the medicine, industry, fiber optic communication, information technology, and consumer electronics. In the military application, it uses in the radar, guidance system of Rocket (bullet) and defense system. This is due to the laser's advantages as previously mentioned in chapter one[27]. In this work, a new model will be designed of free electron laser defenses system FELDS to destroy any target at range 70 Km of sea level.

Free electron laser (FEL) provides coherent radiation, with high power. Also, it can be obtained any wavelength up to ultraviolet and x-ray wavelengths, by using electron gun with high energy. The difference between conventional lasers and Free-electron laser (FEL) is using the relativistic electron beam as a laser medium instead of the active laser medium in the FEL. As previously mentioned the main advantage of FEL is the tunability of the laser beam compared with chemical or CO_2 lasers. Through this feature, it can change the laser wavelength to fit the application [47].

2.1.2 Principle of the free electron laser (FEL)

To generate coherent radiation in a FEL by letting a relativistic electron beam pass through between plates of magnets, these plates are separated by few millimeters, this plate is called wiggler or " undulator". The Lorentz force effects on the electrons when they travel through the wiggler makes the electrons oscillating around the propagation axis. As a result of this oscillating, the emission of laser photon occurs.

The FEL oscillator includes four basic ingredients of an electron gun, electron accelerator, a static periodic magnetic-field (undulator) and an optical resonator as shown in figure (2.1)[48]. The interaction between these elements produces stimulation to oscillate within the optical resonator, and then grows to produce a coherent beam.
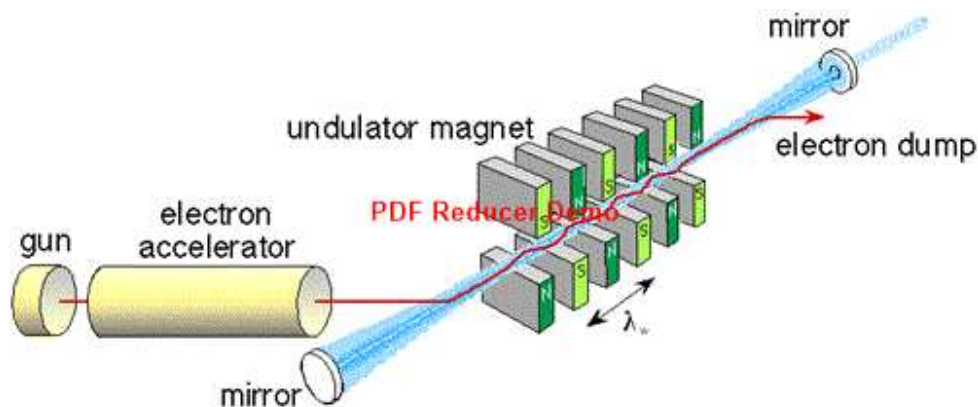
Figure (2.1) The Basic Ingredients of FEL [48].

The accelerator produces an electron beam traveling at relativistic speeds near the light speed. The electron beam is accelerated by an accelerator to approach the speed of light, and then the beam moves toward the wiggler and experiences

regular transverse accelerations due to the periodic magnetic field strength and direction. As the electrons pass from the influence of one magnetic element to the next, the magnetic field bends its paths, causing them to accelerate and emit radiation. Produced by this stimulated emission of radiation is at a wavelength (λ).

From resonance condition, in the undulator, the laser wavelength it can be determined as in equation [43,49]:

$$\lambda = \lambda_m \left(\frac{1}{2\gamma^2} + \frac{K^2}{4\gamma^2} \right) \tag{2.1}$$

Where (γ) the relativistic Lorentz-factor:

$$\gamma = E_{beam}/m_e c^2 \tag{2.2}$$

Where (E_{beam}) is the electron beam energy, (c) is the speed of light equals $3x10^8 \, m/sec$, (m_e) electron mass equal $9.1x10^{-31} \, kg$. And (K) the undulator parameter is determined by:

$$K = \frac{e \, B_w \, \lambda_m}{2\pi \, m_e c} = 0.934 \, B_w \, \lambda_m \tag{2.3}$$

Where (λ_m) the undulator period length in the unit of centimeter, B_w is the intensity of magnetic field of undulator in the unit of Tesla.

The number of undulator periods (N_u) at distance (Z_w) a long undulator can be determined by [47]:

$$N_u = \frac{Z_w}{\lambda_m} \tag{2.4}$$

From the relation between wavelength and electron energy ($\lambda \propto \frac{1}{E_{beam}^2}$), it can be tuning the wavelength over a wide range with the small modification to the

energy of the electron, when the electrons and the radiation propagate through the undulator, the laser power out from undulator (P_z), can be determined by the following equation [45,47,50]:

$$P_z = N_{PH} P_0\, e^{Z_w/L_G} < P_{sat} \qquad (2.5)$$

Where (N_{PH}) the number of coherent photons per electron as expressed in equation 2.7,(P_{sat}) the power after passing a distance (Z_w) through the undulator, (L_G) the gain-length which expressed in the equation 2.9 [50]. And (P_0) is the initial power is the integrated shot noise incoherently radiated into the dominant growing mode by the electrons passing through the first gain length, the initial power can be determined by equation [51,52]:

$$P_0 = \frac{1}{9} \frac{\chi^2 c\, E_{beam}}{\lambda} \qquad (2.6)$$

$$N_{PH} = \frac{\chi\, E_{beam}}{E_{Ph}} \qquad (2.7)$$

Where (E_{Ph}) the photon energy can be determined by:

$$E_{Ph} = \frac{h\, c}{\lambda} \qquad (2.8)$$

$$L_G = \frac{\lambda_m}{4\, \pi\, \sqrt{3}\, \chi} \qquad (2.9)$$

Where (χ) is the scaling parameter of FEL where values of (χ) change from $(10^{-2} - 10^{-3})$ and less for a visible or ultraviolet and defined as [43, 46,51]:

$$\chi = \sqrt[3]{\left(\frac{a_w \, w_p}{4\gamma \, w_c} \, F(k)\right)^2} \qquad (2.10)$$

Where (a_w) the dimensionless vector potential of the undulator, w_p is the plasma frequency of the beam and $F(k)$ is undulator-radiation coupling factor. which are expressed in the equation 2.12, 2.13 and 2.16 respectively and (w_c) is the central-frequency of the emitted radiation and defined as:

$$w_c = \frac{2\pi c}{\lambda} \qquad (2.11)$$

$$a_w = 0.66 \, B_w \, \lambda_m \qquad (2.12)$$

$$w_p = \sqrt{\frac{4 \, \pi \, n_e \, r_e \, c^2}{\gamma}} \qquad (2.13)$$

Where (n_e) is the electron beam density, it is expressed in the equation

$$n_e = \frac{I_{beam}}{2\pi ec(\sigma_x \sigma_y)} \qquad (2.14)$$

Where (I_{beam}) is the beam current, (σ) is the initial beam size, (e) is the electron charge equal $1.6x10^{-19}$ coulombs, (r_e) is the classical radius of the electron defined as [43,46,51]:

$$r_e = \frac{1}{4\pi\epsilon_0} \frac{e^2}{m_e c^2} = 2.817x10^{-15} m \qquad (2.15)$$

$F(k)$ is the undulator-radiation coupling factor and J_0, J_1 are Bessel's functions .

$$F(k) = J_0 \left(\frac{K^2}{(2 + 4K^2)} \right) - J_1 \left(\frac{K^2}{(2 + 4K^2)} \right) \qquad (2.16)$$

The saturation power (power after passing a distance (Z_w) through the undulator) is given by [45,46]:

$$P_{sat} = \chi \, P_{beam} \qquad (2.17)$$

Where (P_{beam}) is the electron beam power and it is given by

$$P_{beam}[MW] = E_{beam}[Mev] \, I_{beam} \, [A] \qquad (2.18)$$

2.1.3 Undulator

The undulator is a mechanical structure consisting of periodic magnets with alternating poles, separated by a distance called (gap). These magnets are made of magnetic material pure permanent magnetic (PPM). The mechanical structure cause's a synchronous radiation. Here used a magnet block of samarium - cobalt (Sm-Co) with dimensions (w=74mm, h=26mm, t=10.5mm) and atomic number for samarium and cobalt is (62,27) respectively and Atomic mass is (150,59), which has a strong resistance to corrosion, oxidation resistance and it can be widely used in high temperature. While the physical properties of samarium-cobalt (Sm-Co) magnets show in Table 2.1 [43,53].

Table 2.1 The physical properties of samarium - cobalt (Sm-Co) magnets [53].

Property	Unit	Value
Magnetic field intensity	Tesla	0.82-1.16
Coercive force (magnetic coercivity)	MA/m	0.493–1.59
Relative permeability	/	1.05
Temperature coefficient of magnetic field	(%/K)	−0.03
Temperature coefficient of magnetic coercivity	(%/K)	−0.15 To –0.30
Curie temperature	(°C)	800
Density	(g/cm^3)	8.2–8.4
Modulus of rupture (bend strength)	(N/mm^2)	150
Compressive strength	(N/mm^2)	800
Tensile strength	(N/mm^2)	35
Electrical resistivity	$(\Omega \cdot cm)$	86×10^{-6}

The relation between the magnetic field of undulator (B_w) , undulator gap (g_w) and undulator period length (λ_m) can be expressed in the equation [43]:

$$B_w = 4.22 \exp\left[-\frac{g_w}{\lambda_m}\left(5.08 + 1.54\frac{g_w}{\lambda_m}\right)\right] \qquad (2.19)$$

2.1.4 Electron beam Injector

The electron injector gun is basically a photocathode that extracts electrons from a metal surface via the photoelectric effect. The electrons emitted from the

injector are accelerated to relativistic velocities (nearly the speed of light) by an electron accelerator. Here we used the beam parameters of the Laser Plasma Accelerators (LPA) facility in SIOM as shown in Table 2.2 [46,54].

Table 2.2 The parameters of the LPA beam for SIOM facility [46,54].

Parameter	Symbol	Value	Unit
Energy of electron beam	E_{beam}	380	Mev
Charge	Q	80	pC
Beam divergence	$\sigma'_{x,y}$	0.1-1	mrad
The electron beam sizes in x directions	σ_x	200	μm
The electron beam sizes in y directions	σ_y	400	μm
Normalized emittance in x directions	ε_x	0.72	μm
Normalized emittance in y directions	ε_y	0.53	μm
Energy spread	σ_δ	1%	/
Beam current	I_{beam}	5.4	kA

2.1.5 Optical Cavity

The optical resonator (optical cavity) used for amplifying the light by using mirrors. The oscillator free electron laser system consists two mirrors the first one (R_1) have reflection one hundred percentages and high reflective for another mirror (R_2). We use concave mirrors with (R_1=100%, R_2 = 98%), separated by a distance(L_c) . The laser resonator configuration show Figure 2.2 [55].

$$L_c$$

Undulator

Fully Reflecting
Mirror

Partially Reflecting
Mirror
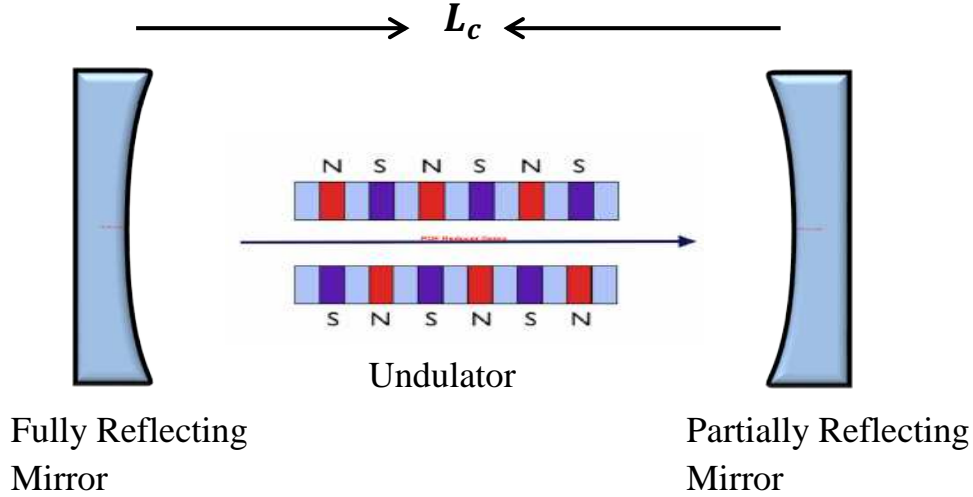
Figure 2.2 shows a typical laser resonator configuration for FEL [55].

2.1.6 The Resonator Stability condition

The Resonator stability condition is very important, must be calculated to maintain the stability of the resonator and grow amplification. The values of R_1, R_2, and L_c determine the stability of resonators, where the radiation coherent is produced by a periodic refocusing of the intra-cavity. If the cavity is unstable, the beam size will grow without limit, eventually growing larger than the size of the cavity mirrors and being lost. The stability of resonator for different types of resonators show in Figure 2. It is possible to calculate the stability criterion by using the equation below[56]:

$$0 < (1 - \frac{L_c}{r_1})(1 - \frac{L_c}{r_2}) < 1 \qquad (2.20)$$

Where $g_1 = (1 - \frac{L_c}{r_1})$, $g_2 = (1 - \frac{L_c}{r_2})$ (where g_1, g_2 is Parameters resonator stability) and r_1, r_2 the radius of curvature for mirror one and two respectively.
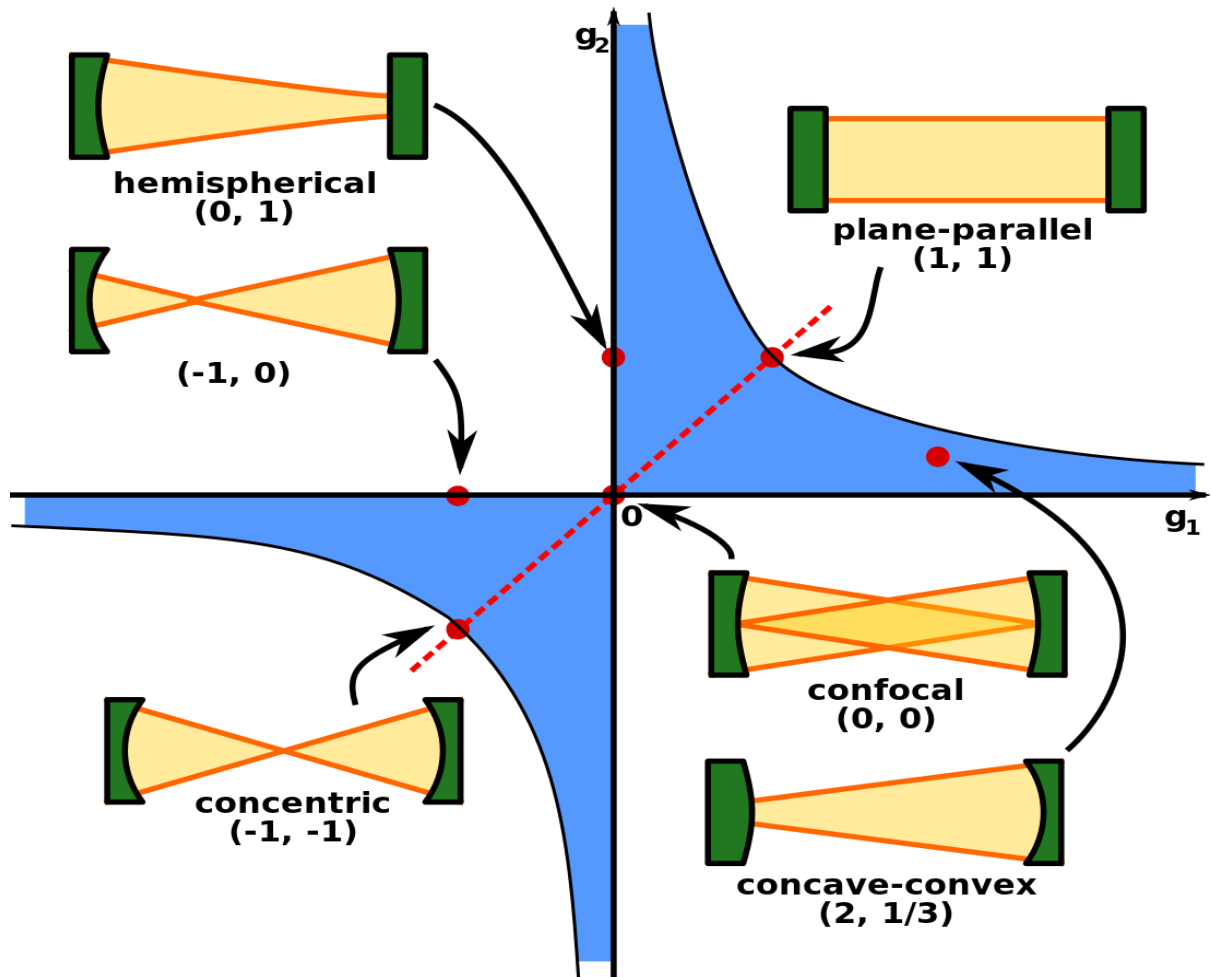
Figure 2.3 shows the diagrams of stability and the radiation pattern inside each cavity for different types of the resonator [56].

Finally, the power of free electron laser defenses system FELDS (out power from the mirror) that amplified by the mirror can by calculated by:

$$P_m = P_z \, R_1 \, R_2 \, e^{2L_c \, (G - \forall)} \qquad (2.21)$$

Where G and $\forall$ is the laser gain and losing parameter respectively, the mirror losing is determined by $\forall = \dfrac{1}{L_c} Ln \, \dfrac{1}{\sqrt{R_1 R_2}}$ [2].

2.1.7 Gaussian Distribution

The power density of laser beam varies depending on the distance or range of targets which is estimated about 70 Km of sea level. The distribution of irradiance in the near field have been as Gaussian distribution and expressed by the following equation [57]:

$$I_{(r,z)} = I_0 \left[\frac{w_0}{w_{(z)}}\right]^2 e^{\frac{-2r^2}{w_{(z)}^2}} \tag{2.22}$$

Where (I_0) is the irradiance at the center of the beam waist ($z = 0$), it reaches to ($1/e^2$) of the maximum value of r is the radial-distance from the optical axis, z is the distance along the optical axis, ($w_{(z)}$) is the radial distance. The ideal Gaussian beam show in Figure 2.4 [57].
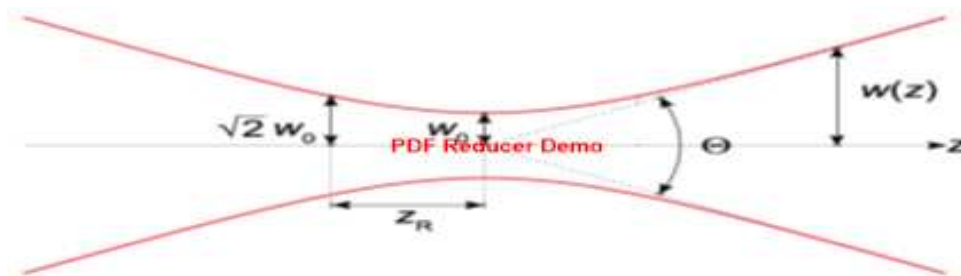
Figure 2.4 shows the ideal Gaussian beam from plot of the $w_{(z)}$ values as a function of z **[57].**

2.1.8 Rayleigh length

In laser science, the Rayleigh-length is an important parameter which is defined as a distance where the curvature of the beam has reached a minimum, or as a distance along the propagation direction of a beam from the waist to the place where the area of the cross section is doubled. The Rayleigh length Z_R and optimal waist radius ω_0 of a Gaussian beam are related to the radiation wavelength λ and the undulator period length λ_m by an equation below [2,20]:

$$Z_R = \sqrt{\frac{g_1 g_2 (1 - g_1 g_2) L_c^{\,2}}{(g_1 + g_2 - 2g_1 g_2)^2}}$$

<div align="right">(2.23)</div>

$$\omega_0 = \sqrt{\frac{\lambda \, Z_R}{\pi}}$$

<div align="right">(2.24)</div>

With Note, the beam expands up to $(\omega_0 \sqrt{2})$ at the end of undulator, the beam cross-section (A_{beam}) is defined as:

$$A_{beam} = 2\,\omega_0^{\,2}$$

<div align="right">(2.25)</div>

The beam spots are much wider in the resonator mirrors. The beam spot size that is out from mirror $d_{(mirror)}$ can be determined by the equation [2]:

$$d_{mirror} = d_0 \sqrt{[1 + \left(\frac{L_c}{2\,Z_R}\right)^2]}$$

<div align="right">(2.26)</div>

Where d_0 is the diameter of beam waist and equals to $2\omega_0$, L_c is the length of the optical resonator (the distance between two mirrors) and Z_R is Rayleigh - length.

2.1.9 M² factor

The output beam from free electron laser is not actually Gaussian. The quality-factor (M^2) is used to measure the difference between an actual beam and a theoretical Gaussian. In the ideal case, the laser beam is exactly Gaussian beam when $M^2 = 1$, but not exactly Gaussian when its value of $M^2 > 1$. The quality-factor M^2 can be calculated by using Rayleigh length as shown in the following equation [58,60]:

$$M^2 = \frac{\pi \, \omega_0^{\,2}}{Z_R \, \lambda}$$

<div align="right">(2.27)</div>

2.2 Standard Atmosphere Modeling

The atmosphere is divided into five layers based on temperature changes with height. These changes are due to solar energy absorption by atmospheric molecules, it moves downward through the atmosphere, the first layer is called the troposphere, this layer extends from 0 km to 11 km, it contains 78.09 % Nitrogen gas, the temperature degree decreases with altitude.

The second layer is called the stratosphere, this layer extends from the altitude 11 km to 50 km, it contains Oxygen 20.95%, it can be divided according to temperature changes with height;

- From 11 km to 20 km the temperature remains constant with increasing height.
- From 20 km to 32 km the temperature degree start increasing with altitude, this increase occurs because the Ozone gas (O_3) absorbs ultraviolet radiation (the short wavelengths) coming from the sun, the ozone (O_3) protects us from ultraviolet radiation which can cause sunburn and cancer.
- From 32 to 47 km temperature increases with altitude at a constant rate.
- From 47 to 50 km the temperature decreases with altitude.

The Third layer is called the Mesosphere, this layer extends from 50 Km to 80 Km, it contains Argon gas 0.93%. The Fourth layer is called the Thermosphere, this layer extends from 80 km to 700 km, it contains Carbon Dioxide 0.039%. The Fifth layer is called the Exosphere, this layer extends from 700 km to 10,000 km, in this layer the water vapor constitutes a proportion 0.4 - 1 %. Table 2.3 shows the temperature changing rate as a function with various altitudes. To calculate the amount of temperature T_A, pressure P_A and density ρ_A

as a function of the altitude, the Standard-of-Atmosphere model can be used. The temperature degree at any altitude is given by below equation [61-64]:

$$T_A = T_{\text{base}} + R_A L_{rate} - R_{base} L_{rate} \tag{2.28}$$

Where (T_{base}) the temperature at the base of the layer, (L_{rate}) is the change in temperature rate, R_A the Altitude in meters, R_{base} is the altitude at the base of the layer in meters. The pressure at the troposphere can be calculated by:

$$P_A = \frac{P_{\text{base}}}{\left[1 - 0.0065 \frac{R_A}{T_{\text{base}}}\right]^{-5.2561}} \tag{2.29}$$

Where (P_{base}) is the Pressure at the base of the layer, the unit of T_{base} is Kelvin and R_A in meters. The pressure above the troposphere can be calculated by:

$$P_A = P_{\text{base}} \exp\left[\frac{-gR_A + gR_{base}}{r_{gas} T_{\text{base}}}\right] \tag{2.30}$$

Where (r_{gas}) is the real gas constant for air $(287.04 \ m^2/K.sec^2)$, g is acceleration of gravity $(9.8 \ m/sec^2)$. From the equation of the temperature, pressure and the density in the altitude R_A can be calculated from the perfect gas equation [61-64]:

$$\rho_A = \frac{P_A}{r_g [T_{\text{base}} + R_A L_{rate} - R_{base} L_{rate}]} \tag{2.31}$$

Table 2.3 shows the temperature changing rate as a function with various altitudes [64].

R_A the altitude in (km)	L_{rate} (K/km)	T_{base} (K)
0	-6.5	288.150
11	0	216.650
20	+1	216.650
32	+2.8	228.650
47	0	270.650
50	-2.8	270.650
70	-2	217.450

2.3 Atmospheric Attenuation

When the laser beam is spread through the atmosphere, its intensity will undergo various attenuation processes as a result of its interaction with the air molecules and water vapor, causing a loss in the power of the laser beam. The laser beam path changes as a result of the difference in the refractive index between the layers of the atmosphere.

In this section, a detailed review of all laser beam attenuation processes will be performed as the beam moves from source to targets, such as scattering and turbulence.

2.3.1 Scattering Attenuation

Atmospheric scattering occurs due to the interaction between laser beam with the atoms and the molecules of the air, the scattering coefficient leads to create an angular redeployment of the radiance component. The atmospheric scattering coefficient (β_{Sc}) in unit $(1/km)$ can be determined by equation [43,63,66]:

$$\beta_{Sc} = \frac{3.912}{R_A} \left[\frac{5500}{\lambda} \right]^V \qquad (2.32)$$

Where λ is laser wavelength in angstrom $(\lambda = 9731\ A^0)$, The value of (V) depends on the range of laser beam, as shown below[44,65,67].

- $V = 0.585(R_A)^{1/3}$ $for\ altitude\ \ (R_A \leq 6\ km)$
- $V = 1.3$ $for\ altitude\ \ (6\ km < R_A < 50\ km)$
- $V = 1.6$ $for\ altitude\ \ (R_A > 50\ km)$

2.3.2   Snow Attenuation

The attenuation affected by the snowflake size and snowfall rate. The size snowflakes are larger than a raindrop, so it causes the significant loss in the laser power. However, the size of snowflake can reach to 20mm, this is an obstacle to the laser beam path as compared to the width of laser beam.

The snow-attenuation can be classified into dry snow attenuation and wet snow attenuation. The snow attenuation coefficient (β_{Sn}) in unit $(1/km)$ can be determined by equation [40,69]:

$$\beta_{Sn} = aS^b \qquad (2.33)$$

Where S is the snow rate in millimeters/hour, (a) and (b) is the value of dry and wet snow, it's given by relation below:

For wet snow (altitude < 0.5 Km):

$$a = 1.023\ x10^{-5}\ \lambda + 3.785\ and\ b = 0.72 \qquad (2.34)$$

For dry snow (altitude ≥ 0.5 Km):

$$a = 5.42\ x10^{-6}\ \lambda + 5.495\ and\ b = 1.38 \qquad (2.35)$$

where the wavelength of laser λ in Angstrom (A^0).

2.3.3 Rain Attenuation

The large rain droplets can cause losing in laser power, the attenuation of rainfall increases linearly with rainfall rate. The rain attenuation coefficient (β_{ra}) in unit $(1/km)$ can be determined by equation [40,69]:

$$\beta_{ra} = 1.076\ R_{ra}{}^{0.67} \qquad (2.36)$$

where R_{ra} is the rainfall rate in millimeters/hour.

2.3.4 Atmospheric Turbulence

Atmospheric turbulence occurs as a result of the random change of temperature in the successive atmosphere layers. This change in temperature leads to changes in density, and as a result, the refractive index changes and the laser beam deviates at a certain angle from its original path according to the SNELL law [42].

2.3.4.1 Air Refractive-Index

The refractive-index is generated by changes in density or change in the temperature of air in the atmosphere layers. Where the refractive-index of the

atmosphere is a function of temperature, pressure, and wavelength. The refractive index can be calculated by [62]:

$$n = \left[1 + \frac{77.6 \text{ x} 10^{-6} \, P_A}{T_A}\right]\left[1 + \frac{7.53 \text{x} 10^5}{\lambda^2}\right] \qquad (2.37)$$

2.3.4.2 Index of refraction structure factor C_n^2

Another important parameter is the refractive structure factor C_n^2 (m$^{-2/3}$) defined as the mean-square difference in the refractive index at two locations divided by the scalar distance r raised to the 2/3 power. The C_n^2 used to determine the strength of the turbulence in the atmosphere layers. The first amount of theoretically parameterized has been measured at several locations worldwide was Andrey Kolmogorov. The theory of Andrey Kolmogorov statistical methodology is used in characterization of the kinetic energy flow from large-scale eddy (ten of meters) to small-scale eddy (centimeter) in size. Eddy is a range of sizes relatively homogeneous and isotropic within smaller regions of space. Kolmogorov determined the value of turbulence in the different altitudes by using the following relation[30,42,70,71]:

$$C_n^2 = \frac{\langle (n_2 - n_1)^2 \rangle}{r_i^{2/3}} \qquad (2.38)$$

Where r_i represents a scalar distance between areas.

Table 2.4 shows the value of refractive structure factor C_n^2 for various atmospheric conditions [30,42,70,71].

$C_n^2 \; (m^{-\frac{2}{3}})$	Atmospheric turbulences
$C_n^2 \geq 10^{-12}$	Strong-Turbulence

$10^{-12} > C_n^2 > 10^{-17}$	Medium-Turbulence
$C_n^2 \leq 10^{-17}$	Weak-Turbulence

2.3.4.3 Fried Parameter r_0

Another important value is used to describe the turbulence of the beam propagation in the atmosphere layers called the Fried-Parameter(r_0), which represents the Coherence diameter in atmospheric. The r_0 parameter is a circular diameter of the laser beam which preserves coherence in the propagation-distance. If the value of r_0 is lower, it means a stronger turbulence, and vice versa. The Fried-parameter (r_0) depends on Index refraction structure parameter (C_n^2), the wavelength of laser (λ) and the distance to the target, the value of r_0 can be calculated by the equation [70]:

$$r_0 = 0.33 \, \lambda^{6/5} \left[R_A^{\frac{3}{5}} \left(\frac{[(n_2 - n_1)^2]}{r_i^{\frac{2}{3}}} \right) \right]^{-3/5} \qquad (2.39)$$

Chapter Three
Design and Simulate of Free Electron Laser Defenses System FELDS

CHAPTER THREE

Design and Simulate of Free Electron Laser Defenses System FELDS

3.1 Introduction

In this chapter, a new model of free electron laser defenses system FELDS is designed in infrared range with high out power to destroy any target (missile, aircraft) at range 70 Km.

Through simulation, the atmospheric effect on the laser beam (such as absorption, scattering, fog, rain, reflection index and beam diverges) was analyzed and calculated.

3.2   The Design of FELDS

The design of any defense system requires knowledge of the characteristics of the target, the altitude of the target and its movement whether directed towards the defense system or away. As long as the target is defined as a missile or aircraft, many factors affecting on the attenuation of the laser beam must be calculated in order to determine the amount of the power of FELD and the lost power in the atmosphere. All these factors, as well as other factors will be explained in detail in this chapter.

A new free electron laser defenses system FELDS was designed as shown in Figure 3.1 and 3.2. In this design, the undulator period length about (5.6 cm), undulator gap (15.61 mm), undulator magnetic field intensity (1.1541 Tesla) and

using electron energy beam (380 MeV), all these parameters was calculated to obtain a laser beam with wavelength (9731 A^0) based on Eq. (2.1) – (2.3).

The laser power depends on the electron energy beam, undulator length and the power amplifier by the resonator. So to reach power (15.49 GW), will be used an undulator with length (2.5 m) based on Eq. (2.5) to Eq. (2.18). All the basic information and parameters of the FELDS design are shown in the table.
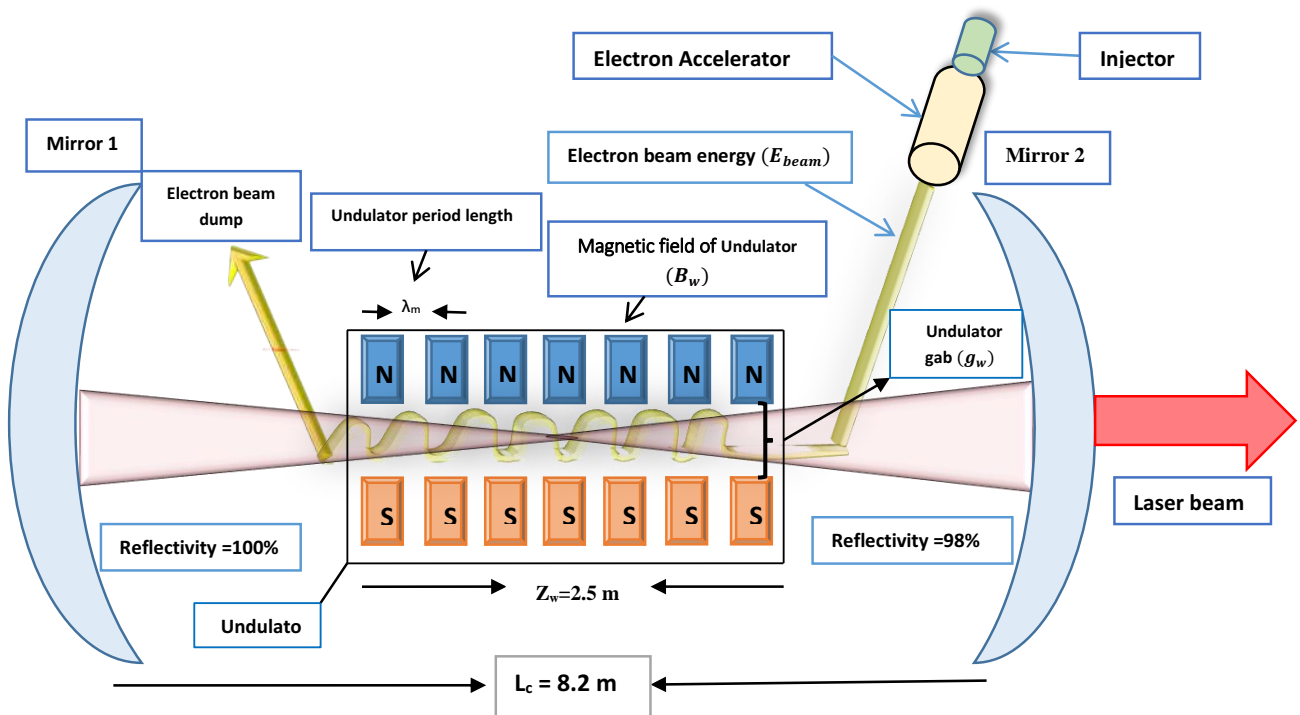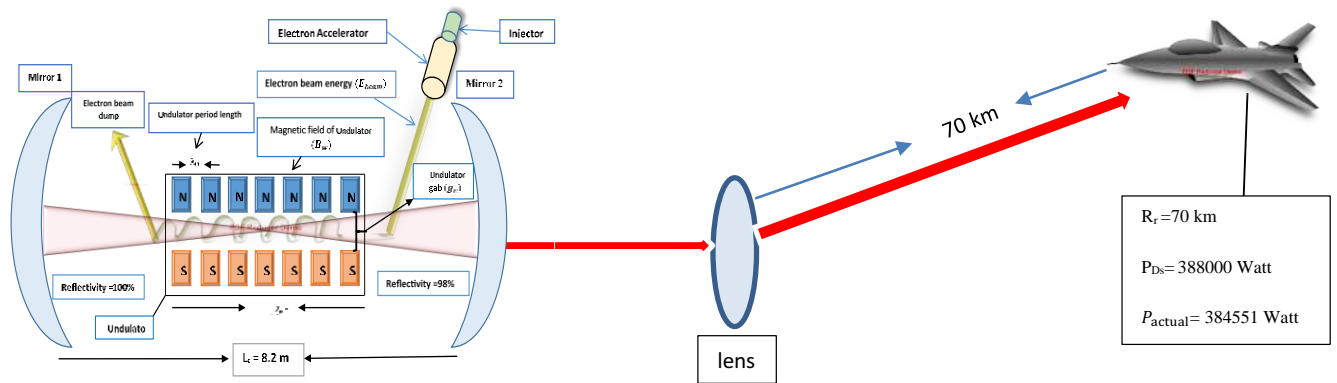
Figure 3.1 shows the FELDS design.

Figure 3.2 shows the mechanism of FELDS.

Table 3.1 shows the parameters of FELDS.

Parameters	Amount	Unit
Electron beam energy (E_{beam})	380	MeV
Radiation wavelength (λ)	9731	A^0
Undulator period length (λ_m)	5.6	cm
Magnetic field of undulator (B_w)	1.1541	T
Undulator gap (g_w)	15.61	mm
Undulator parameter (K)	6.036	/
FEL parameter (χ)	$1.51 x 10^{-3}$	/
Power gain length (L_G)	1.69	m
The saturation power (P_{sat})	3.11	GW
Laser power (P_Z)	9.4	kW
Undulator Length (Z_w)	2.5	m
Relativistic factor (γ)	743.63	/
Number of undulator period (N)	44	/
Number of electron in beam $(N_{electron})$	451474	/

3.3 The Design of Resonator

The design of FELDS resonator contains two mirrors separated by a distance equal to (8.2 m), each mirror has radius (4.11 m). The reflectivity of the first mirror (100%) and the second mirror (98%) in order to obtain power about (15.49 GW). Table 3.2 shows the optical resonator (optical cavity) parameters of the free electron laser FELDS, these parameters were calculated based on Eq. (2.20) to Eq. (2.26).

Table 3.2 shows the optical resonator (optical cavity) parameters of FELDS.

Parameters	Amount	Unit
Mirror material	Au/Cu	
Distance between two mirrors (L_c)	8.2	m
The reflectivity of mirrors (R_1)	100 %	/
The reflectivity of mirrors (R_2)	98 %	/
the radius of mirrors (r_1, r_2)	4.11	m
Resonator stability (g_1)	-0.995	/
Resonator stability (g_2)	-0.995	/
Resonator stability $(g_1\ g_2)$	0.99	/
Rayleigh length (Z_R)	20.2	cm
waist radius (ω_0)	0.25	mm
Beam radius (d_{mirror})	10.15	mm
The quality-factor (M^2)	0.998	/
The gain parameter (G)	1	m^{-1}
Losses parameter $(\forall)$	0.126	m^{-1}
laser power at mirror (out power) (P_m)	15.49	GW

In order to simulate the defense system, and estimate the parameters of that system, a special program was established using the language visual basic software 2010, which contains many parameters as shown in Fig 3.3.
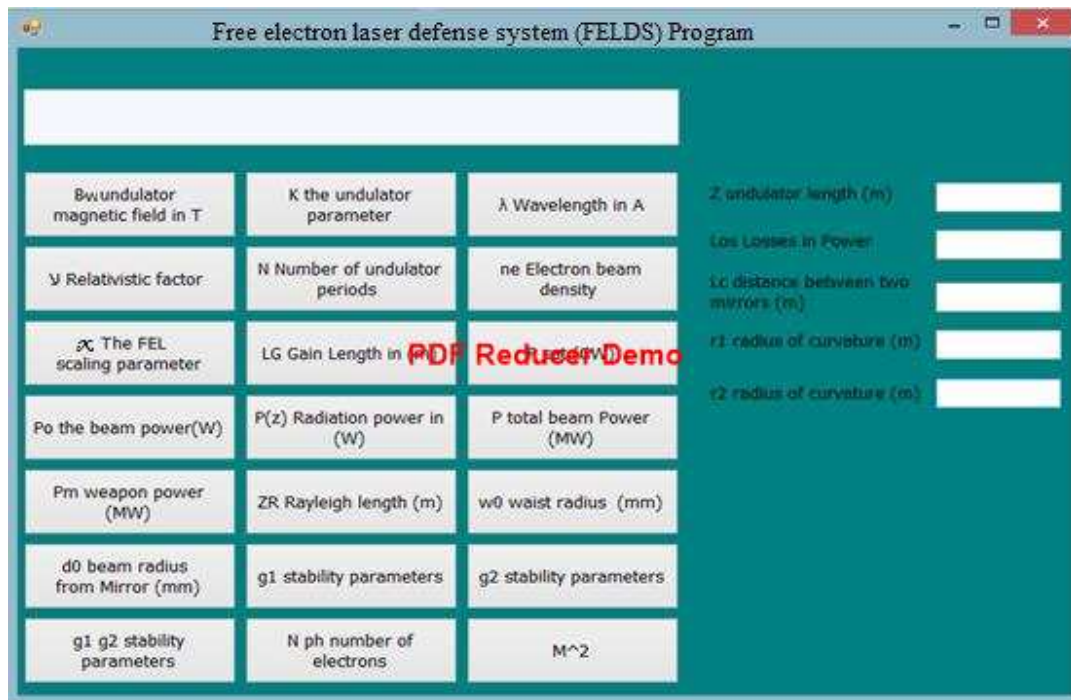

Figure 3.3 shows the design of FELDS program.

3.4   Calculating the affect parameter on the FELDS
In this section, basic equations will be presented to estimate the atmosphere effect on the FELDS power. Also, the important parameters were presented to calculate the power needed to destroy the target.

3.4.1 The reached power
The power of the laser beam undergoes various attenuation processes as it passes through the different atmospheric layers as described in the previous chapter. The power of the FELDS reaching the target was calculated based on Beers-Lambert Law as shown in eq. (3.1) [70].

$$P_{Ds} = P_m \, e^{-\beta R_r} \tag{3.1}$$

Where (P_{Ds}) is the laser power on target, (P_m) is the laser power at mirror (real power), (β) is the total attenuation (rainy, scattering, snowfall) in (1/km) , (R_r) is the target range in (km) [35,72,73]:

$$\beta = \beta_{sc} + \beta_{sn} + \beta_{ra} \tag{3.2}$$

3.4.2 The Extra Distance of Target

Although the laser beam moves at the speed of light and thus greatly limits target maneuverability, this feature is very important and is not available in conventional weapons. But in order to locate the target with high accuracy the extra distance (D_{ta}) of the target must be calculated.

The extra distance (D_{ta}) represents the distance traveled by the target during the time period between the moments of launch of the laser beam from the FELDS to the moment it falls on the target. It can be calculated by:

$$D_{ta} = \frac{v_{ta} \, R_r}{c} \tag{3.3}$$

Where v_{ta} the speed of the target in m/sec, (R_r) the range of target in mater, (c) the speed of light equals to $3x10^8 \, m/sec$ and the (D_{ta}) distance in mater [18].

3.4.3 Laser Beam Divergence

The turbulences in atmospheric layers have an effect on the spot size of the laser beam. The Free electron laser beam can be accurately modeled as a Gaussian beam, the increase in spot size is called Beam Divergence (δ). It can by calculated by the equation [70]:

$$\delta = \frac{\lambda \, R_r}{\pi \, d_{mirror}} \tag{3.4}$$

3.4.4 The Power Needed and Target Characterization

The amount of the power needed to destroy any target is determined by the total energy delivered per unit area (F). It's depended on several factors such as the dwell time (the time that a laser beam spends on a target), the properties of the target material and the thickness of skin target. The intensity (Γ), on the target is defined as [19,29,54]:

$$\Gamma = \frac{P_{Tm}}{A} \tag{3.5}$$

Where (P_{Tm}) the power needed for destroying the target is made from steel or aluminum without the reflectivity, (A) is the cross sectional area of the beam spot on the target expressed by equation (3.6). (F) on target is obtained from the time integral of the intensity [20,30,55]:

$$A = \frac{\lambda^2 R_A{}^2}{\pi \, \omega_r{}^2} \tag{3.6}$$

$$F = \int_o^t \Gamma \, dt = \frac{P_{Tm} t_{in}}{A} \tag{3.7}$$

From Eq. 3.5 and Eq. 3.6 and Eq. 3.7 can get

$$F = \frac{P_{Tm} t_{in} \pi \, \omega_r{}^2}{\lambda^2 R_A{}^2} \tag{3.8}$$

Where (t_{in}) the dwell time (in this work $(t_{in} = 3 \text{ sec})$) and (ω_r) is radius of laser beam spot.

The total energy required (E_t) to heat a certain section from target up to the melting or vaporizing point can be determined from the equation:

$$E_t = A\rho_m d_t [C(T_m - T_R) + L_m + C(T_m - T_v) + L_v] \qquad (3.9)$$

where (ρ_m) is the density of material, (d_t) is the thickness of the material, (C) is the target specific heat capacity, (T_m) is melting-point of target material, (T_R) is the temperature of the target at altitude R_A , (L_m) is latent heat of melting of target surface, (T_v) is the target vaporizing point, is (L_v) Latent-heat of vaporizing of target surface.

Table 3.3 illustrates the thermal properties of target metals. So, the energy per unit area (F) to destroy the target is:

$$F = \frac{E_t}{A} = \rho_m d_t [C(T_m - T_R) + L_m + C(T_m - T_v) + L_v] \qquad (3.10)$$

From equating equation. 3.8 and 3.10 we can get (P_{Tm}) the power needed for destroying the target:

$$P_{Tm} = \frac{\lambda^2 R_A{}^2 \rho_m d_t}{t_{in} \pi \, \omega_r{}^2} \, [C(T_m - T_R) + L_m + C(T_m - T_v) + L_v] \qquad (3.11)$$

Table 3.3 Thermal properties of target metals [20].

Parameter	Missile	Aircraft
Velocity v_t (m/s)	800-5250	50-350
Surface Material	Steel	Aluminum
Surface Thickness d_t (cm)	0.1-0.3	0.1-0.3
the-specific heat capacity C (J/gm.C^0)	0.452	0.91
Melting point T_m (C^0)	1425	660
Vaporizing point T_v (C^0)	2971	2467
Latent Heat of Melting L_m (J/gm)	250	321
Latent Heat of Vaporizing L_v (J/gm)	6200	10500
Density ρ_m (gm/cm^3)	7.87	2.70
Mass m (gm)	14.75	5.06

3.4.5 The Reflectivity of Skin's Target

Reflectivity is one of the greatest challenges to the development and proliferation of laser weapons systems, where most laser beam power is reflected when it falls on the surface of the target.

As the target surfaces (missile or aircraft) are made of steel or aluminum, which have a high reflectivity for the laser beam, so the laser beam will lose about 90% of its total power [20,30,55].

The actual power (P_{actual}) needed to destroy the target can be calculated by equation below:

$$P_{\text{actual}} = P_{Tm} \left(\frac{1}{100\% - 90\%} \right) = 10 \, P_{Tm} \tag{3.12}$$

Chapter Four
Results and Discussion

Chapter Four

Results and Discussion

4.1 Introduction

In this chapter, all simulations results obtained by creating a multi-parameter program (as described in Chapter 3) will be reviewed. Where it calculated the amount of energy needed to destroy any target within the range allowed, as well as all the weather Parameters that caused a loss in the energy of the laser beam as it moves from the FELDS to the target. As well as other results will be analyzed and discussed in detail based on the physical principle mentioned in Chapter 2.

4.2 The Design of Free Electron Laser Defenses System FELDS

The proposed design of the FELDS, shown in Fig. 3.1, consists mainly of three parts. The important part is the undulator, it will use an undulator with length (2.5 m), which makes the electrons oscillating around the propagation axis. As a result of this oscillating, the emission of laser photon occurs. The radiation spectral width depends on the number of undulator periods. The relation between the undulator period length (λ_m) and wavelength (λ) of laser beam, is represented by the curve as shown in figure (4.1). The wavelength of the laser beam for FELDS depends on the undulator period length (λ_m). As a result of the acceleration and deceleration of the electron as it moves between the poles of the magnet, energy will be emitted in the form of photons, the amount of photon energy proportional to the undulator period length (λ_m).

This process represents the basic principle for determining the wavelength of the transmitted laser beam at (9731 A^0) when the value of electron energy beam(E_{beam}), undulator gap (g_w), and magnetic field(B_w) are constant. This corresponds to the theoretical part (equations 2.1&2.3).
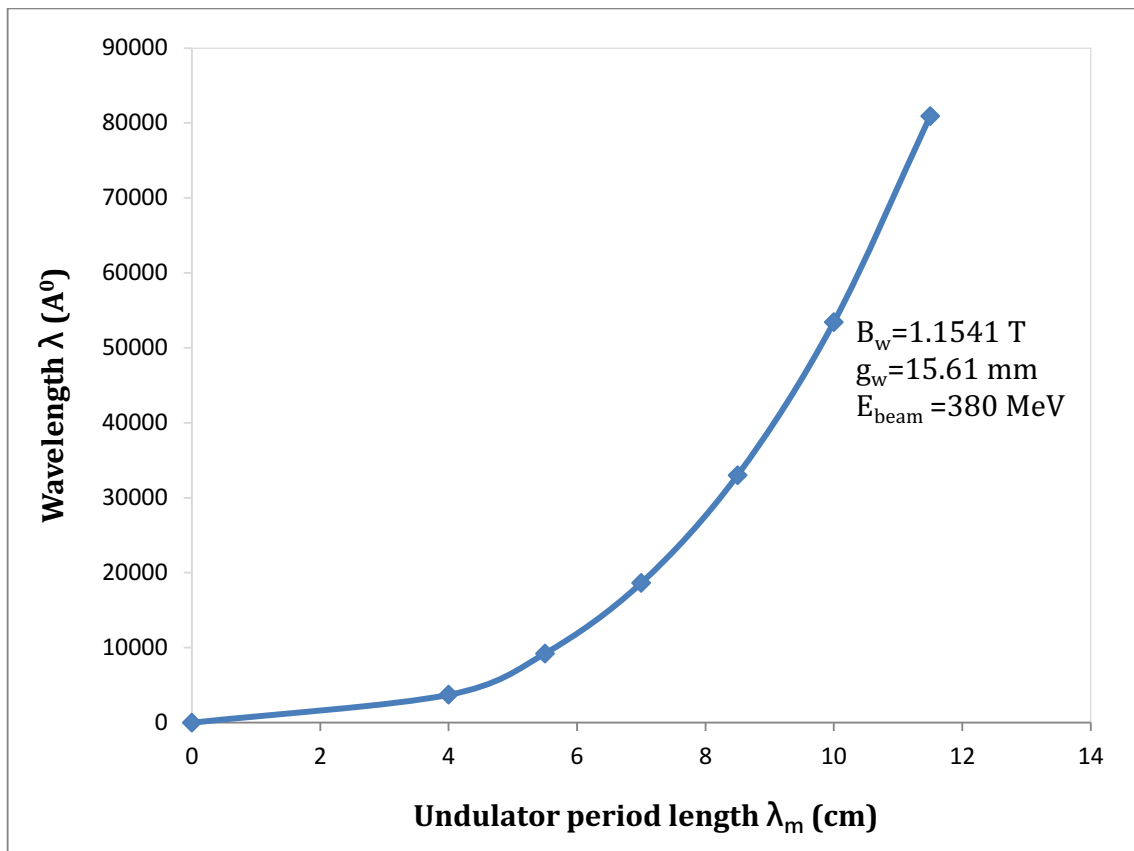

Figure 4.1 shows the wavelength (λ) change with the change of undulator period length (λ_m).

Figure (4.2) shows the inversely proportional between the wavelength (λ) and electron energy beam (E_{beam}) at a constant value for undulator period length (λ_m), undulator gap (g_w), and magnetic field(B_w). That is identical with law of photon energy ($E = hc/\lambda$).
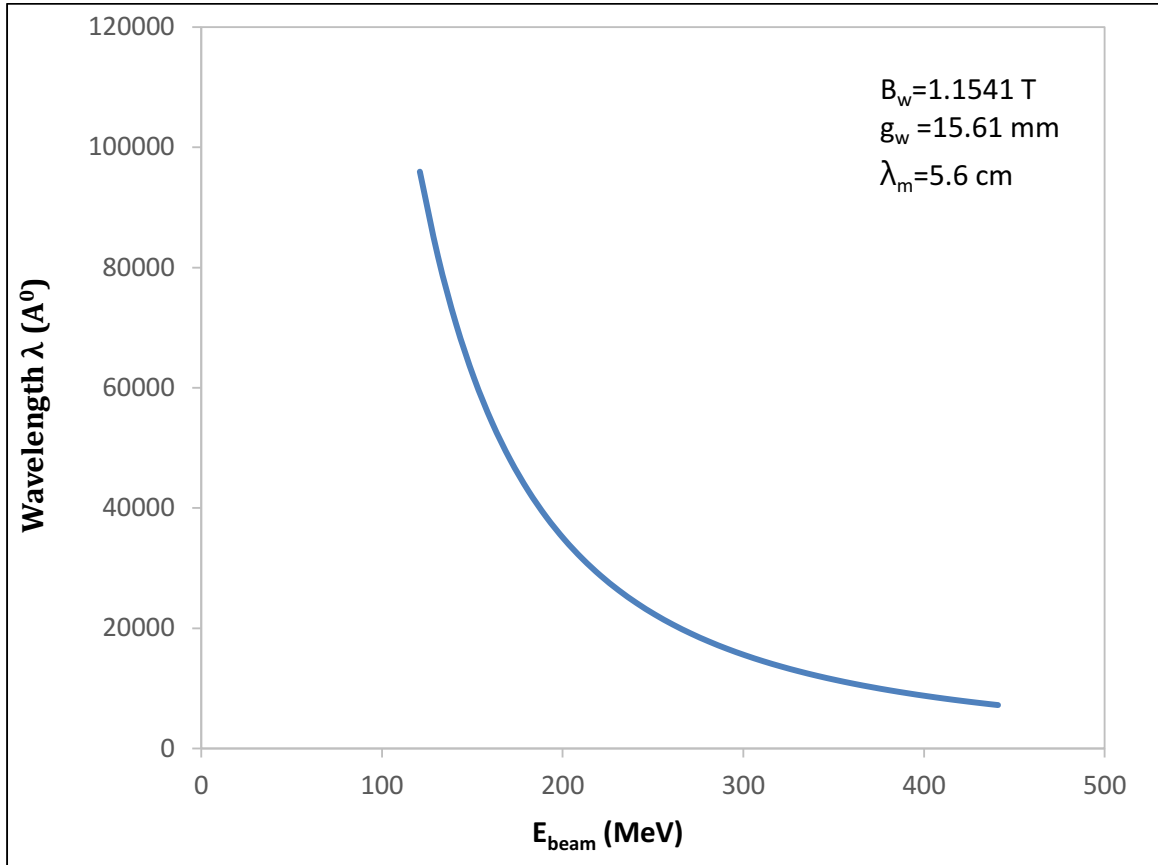
Figure 4.2 shows the inversely proportional between the wavelength (λ) and electron energy beam (E_{beam}).

According to the figure above, it can get any wavelength of the laser by changing these parameters (electron energy beam, undulator period and undulator gap) and this is in agreement with the physical principle.

The Laser power of FELDS (P_Z) depends on the undulator length(Z_w) according to the equation (2.5), the relation between (P_z) and (Z_w) shown in Figure (4.3).
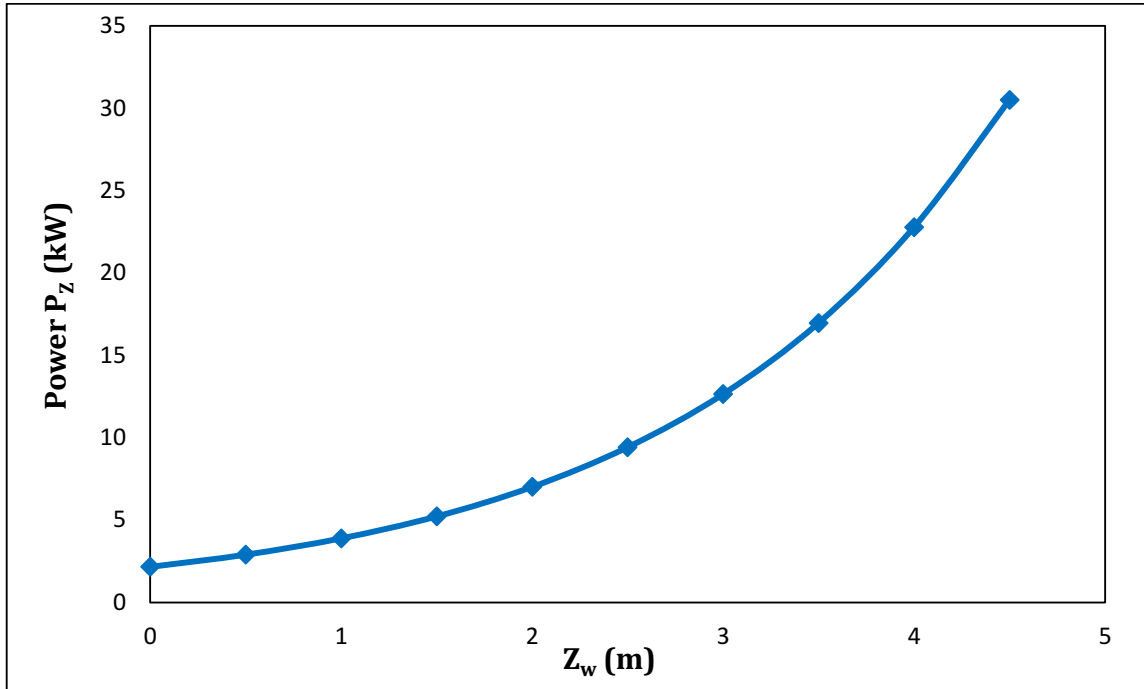
Figure 4.3 shows the directly proportional between the laser power P$_Z$ (kW) and the undulator length Z$_w$ (m).

The amplifier of the laser power (P_m) by the mirror depends on the distance between two mirrors (L_c) and the reflectivity of the mirrors (R_1, R_2), Figure 4.4 shows the effect of distance between two mirrors (L_c) on the amplifier of the laser power(P_m). Where the power (P_m) is directly proportional with distance between two mirrors(L_c), and this is identical with Eq.(2.21). The resonators are used to select frequencies further. The increase of the resonators length will lead to the generation of coherent photons, where the increase of the movement of photons back and forth leads to the stimulation of other photons at the same frequency.
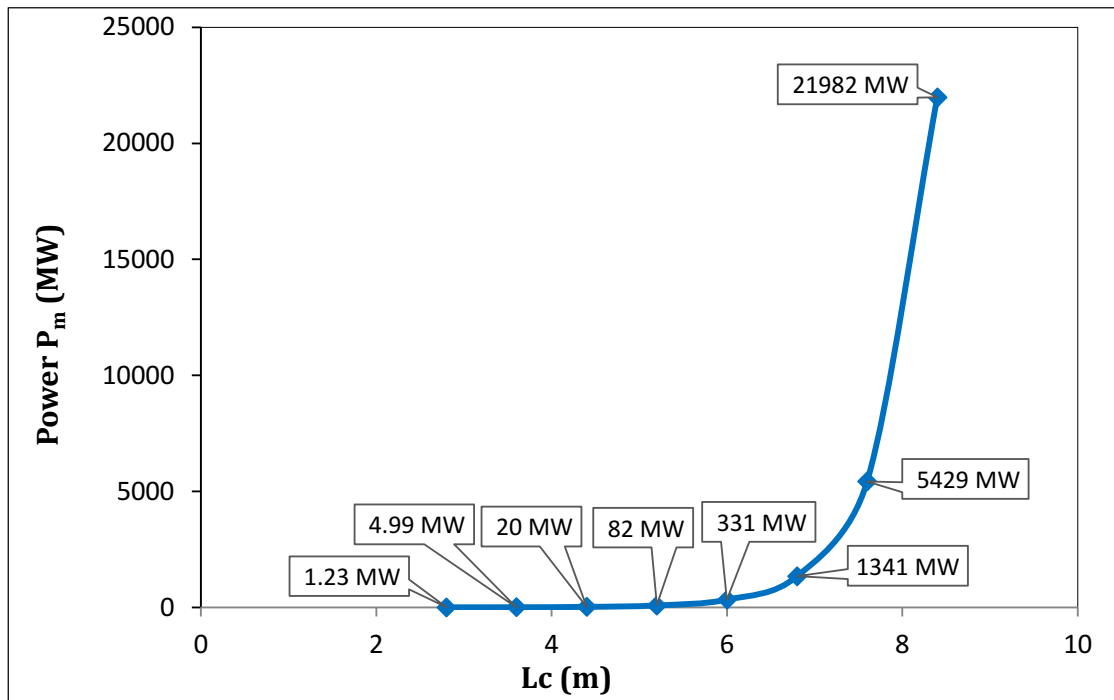
Figure 4.4 shows the effect of distance between two mirrors (L_c) on the amplifier of the laser power (P_m).

The spot size of laser beam which is out from mirror (d_{mirror}) is directly proportional with the distance between two mirrors (L_c) and inversely proportional with the Rayleigh length (Z_R), Figure 4.5 shows the relation between the beam spot size (d_{mirror}) and the distance between two mirrors (L_c). The beam spots are much wider in the resonator mirrors. That's identical with Eq. (2.26). The reason for the large increase in spot size (d_{mirror}) is that the increased distance between the mirrors (L_c) is accompanied by a large increase in the length of Rayleigh (Z_R), this causes an exponential rise in spot size as shown in the curve.
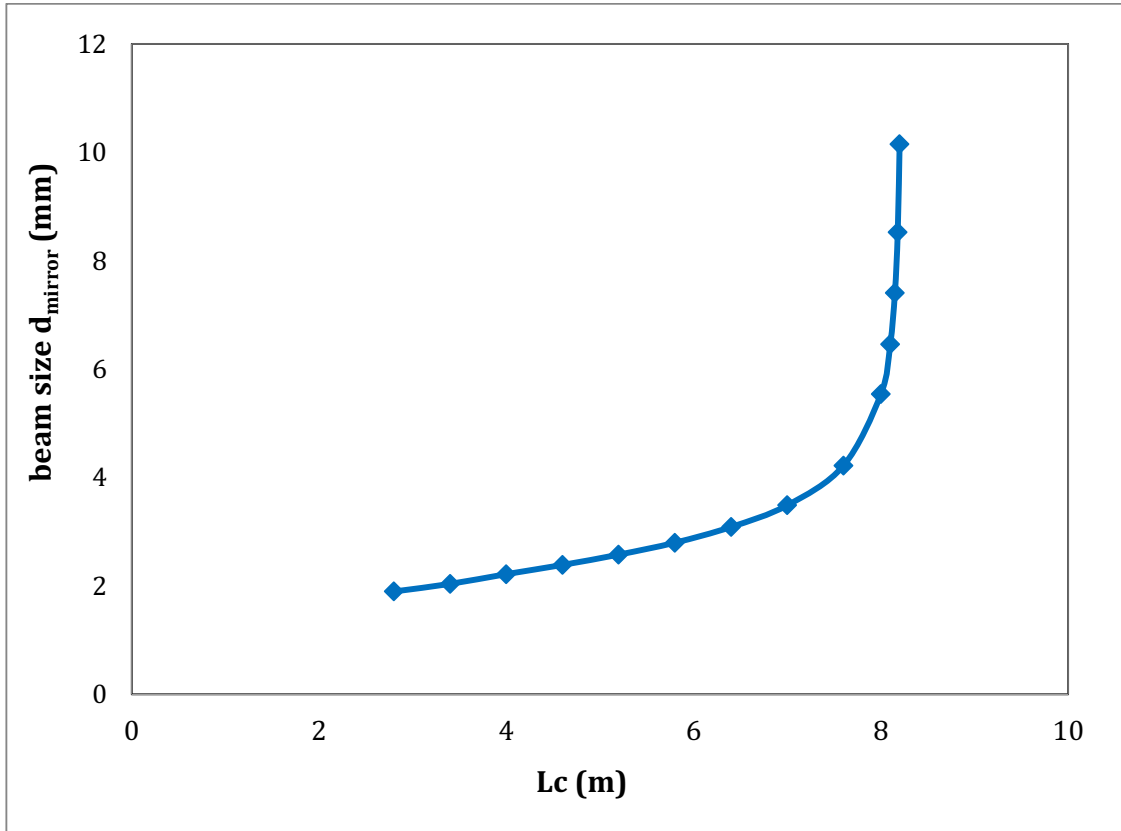
Figure 4.5: Shows the relation between the beam spot size(d_{mirror}) and the distance between two mirrors (L_c).

According to the equation (2.23) the Rayleigh length (Z_R) value depending on the distance between two mirrors (*Lc*) and stability of resonator (g1and g2), where (Z_R) increasing at (Lc) equal to 2.8 to 5.8, above this value of (Lc) (from 5.7 to 8.2) Rayleigh length value decreasing with increasing distance between two mirrors this decrease occurs as a result of the change in the value of (g1 and g2) according to the equation (2.20), figure 4.6 shown the change in the Rayleigh length as a function of distance between two mirrors (Lc).
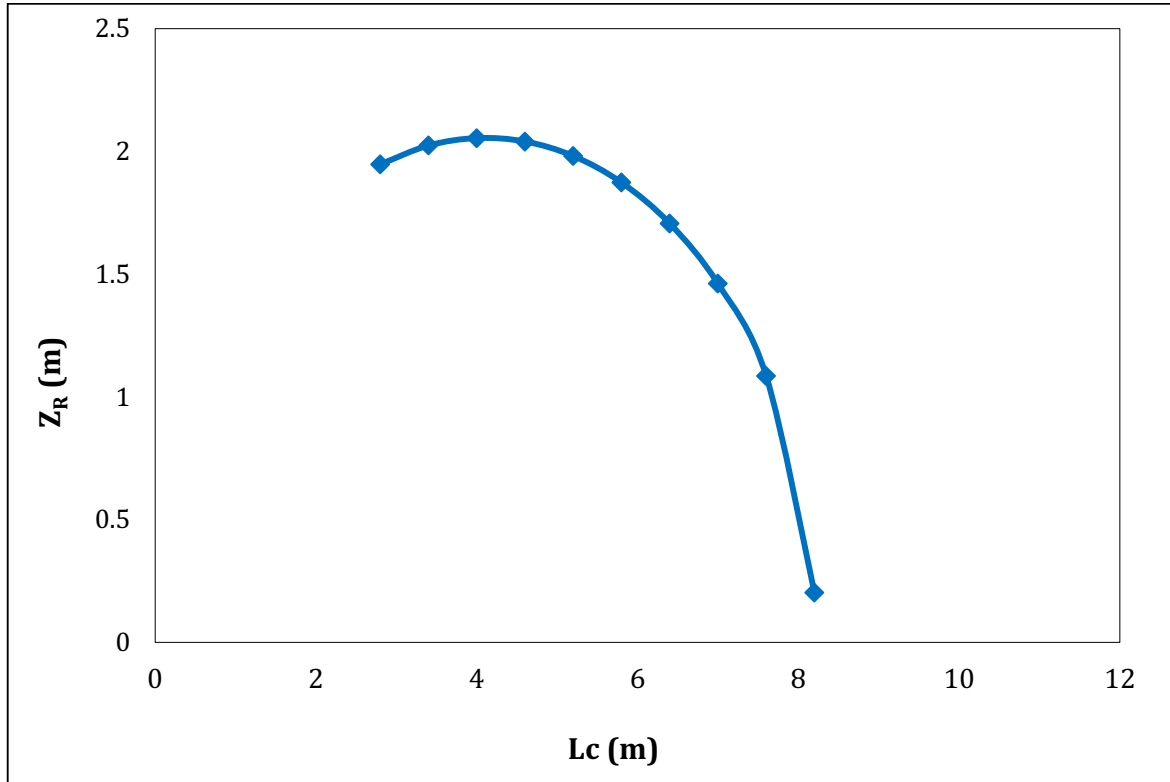
Figure 4.6 shows the relation between the Rayleigh length (Z_R) and the distance between two mirrors (L_c).

4.3   Standard Atmosphere Modeling

Moving away from the earth's surface causes a significant change in temperature (T_A), as a result of the different components of the atmosphere depending on equation (2.28). Also, the pressure P_A(mbar) and density ρ_A (kg/m^3) vary with altitude R_A (km) depending on equations (2.29-2.31). It can show the P_A and ρ_A drops exponentially with increasing altitude above mean sea level because most of the atmospheric mass concentrates in a troposphere layer. Subsequently, this has significant effects on the Laser power depending on the change of temperature (T_A), pressure (P_A) and density (ρ_A). Table 4.1 shows the value of the temperature, pressure and density as a function of altitude.

Table 4.1 shows the value of the temperature, pressure, and density as a function of altitude.

$R_A(km)$	T_A (K)	$P_A(mbar)$	$\rho_A\left(\dfrac{kg}{m^3}\right)$
0	288.15	1013.25	1.225
5	255.65	540.18	0.736
10	223.15	264.34	0.4127
15	216.65	120.45	0.1936
20	216.65	54.78	0.0880
25	221.65	25.359	0.0398
30	226.65	12.145	0.0186
35	237.05	5.926	0.0087
40	251.05	3.075	0.0042
45	265.05	1.710	0.0022
50	270.65	0.942	0.0012
55	259.45	0.490	0.00065
60	245.45	0.237	0.00033
65	231.45	0.105	0.00015
70	217.45	0.042	$6.7x10^{-5}$

The change in the temperature, pressure and density with altitude shown in Figure 4.7, 4.8 and 4.9.
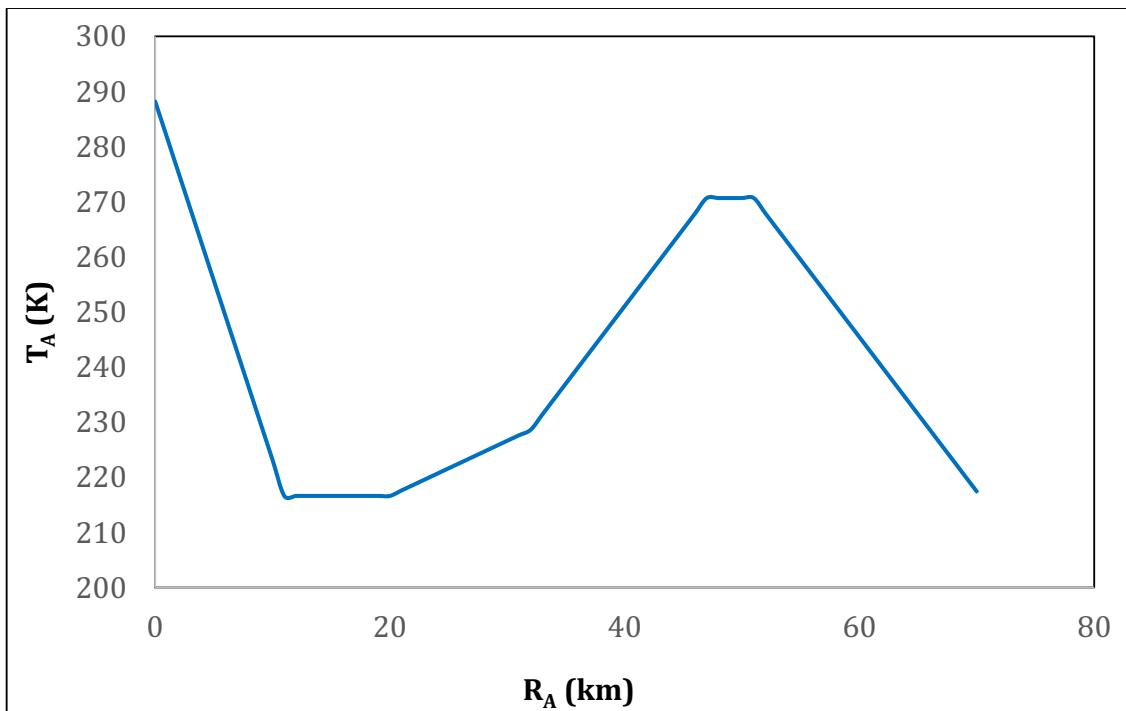

Figure 4.7 shows the change in temperature degree T_A (K) with altitude R_A (km).
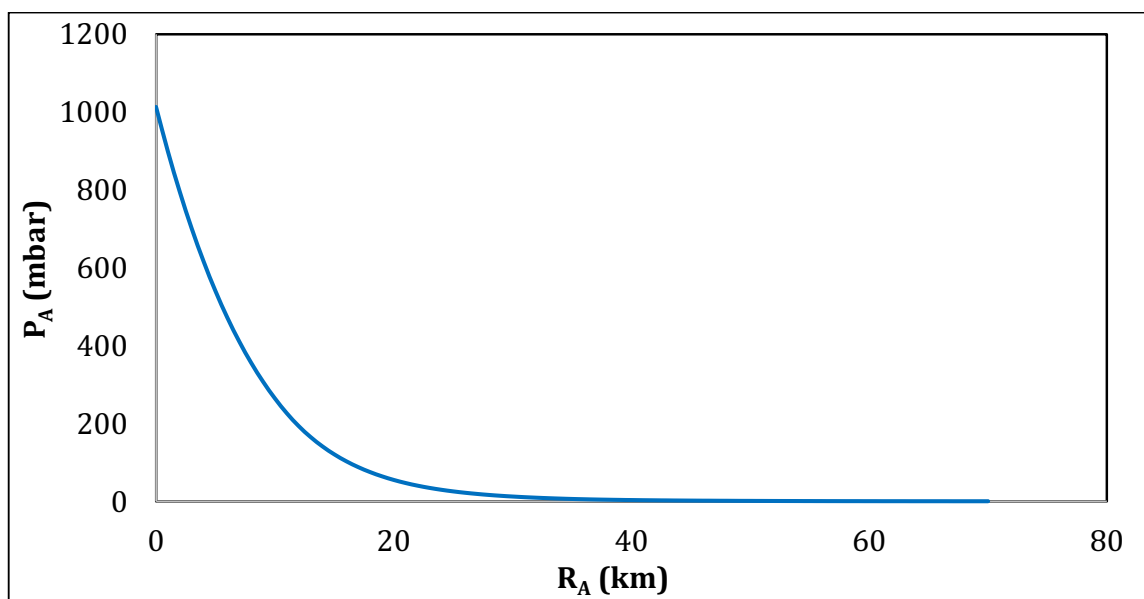

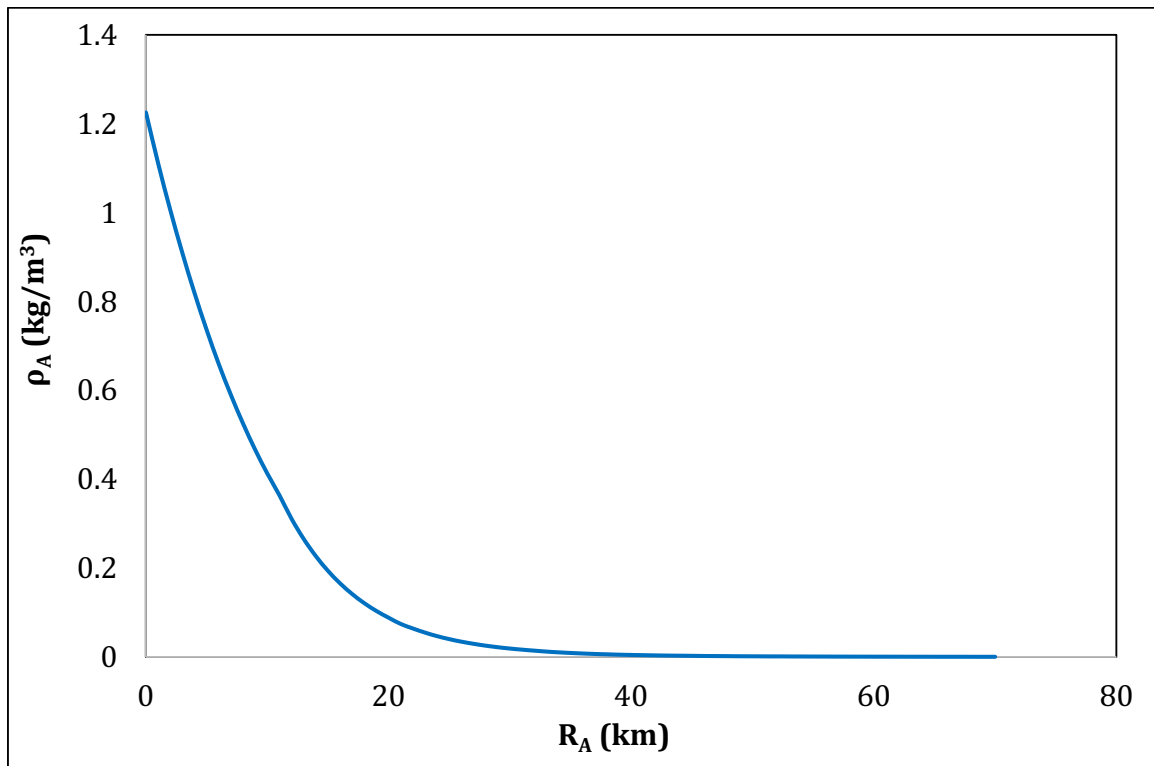Figure 4.8 shows the change in the pressure P_A (mbar) with altitude R_A (km).

Figure 4.9 shows the change in density ρ_A (kg/m³) with altitude R_A (km).

From the figures, we can see the change in temperature (increase, decreases) are due to solar energy absorption by atmospheric molecules, the density and pressure are less valuable in the atmosphere as a result of higher altitude than sea level, these phenomena are due to the most of the basic components of the atmosphere (molecule's, small atoms and aerosol) are concentrated in the troposphere layer.

4.4   Atmospheric Attenuation

The atmospheric attenuation that affects on the FELDS was calculated by using the equations (2.32-2.36). The first layers of the atmosphere (0 - 11 km) have most weather changes caused by the gases and aerosol that are abundant in this

layer. According to equations that mentioned above (2.32-2.36), Table 4.2 shows the value of scattering, snow and rain attenuation that change with altitude.

Table 4.2 shows the value of scattering, snow and rain attenuation that change with range.

R_r (km)	V	$\beta\ (\dfrac{1}{km})$	P_{DS} (KW) without rain & snow	P_{DS} (W) with rain & snow
0	0		$15.49x10^9$	$15.49x10^9$
5	1	0.442	$4.21x10^4$	$3.3x10^2$
10	1.3	0.186	$1.21x10^4$	$7.8x10^{-4}$
15	1.3	0.124	$5.87x10^3$	$3.6x10^{-5}$
20	1.3	0.093	$3.49x10^3$	$2.7x10^{-5}$
25	1.3	0.074	$2.33x10^3$	$1.4x10^{-5}$
30	1.3	0.062	$1.67x10^3$	$1.0x10^{-5}$
35	1.3	0.053	$1.26x10^3$	$7.8x10^{-6}$
40	1.3	0.046	$9.88x10^2$	$6.1x10^{-6}$
45	1.3	0.041	$7.95x10^2$	$4.9x10^{-6}$
50	1.3	0.037	$6.55x10^2$	$4.0x10^{-6}$
55	1.6	0.028	$5.64x10^2$	$3.5x10^{-6}$
60	1.6	0.026	$4.93x10^2$	$3.0x10^{-6}$
65	1.6	0.024	$4.35x10^2$	$2.7x10^{-6}$
70	1.6	0.022	$3.88x10^2$	$2.4x10^{-6}$

Figure 4.10 illustrates the inversely proportional between the range R_r (km) and scattering and absorption coefficient β_{Sc} (1/km).

Also, Fig 4.11 illustrates the inversely proportional between the range R_r (km) and the reach power need to de.stroy the target P_{DS} (W).
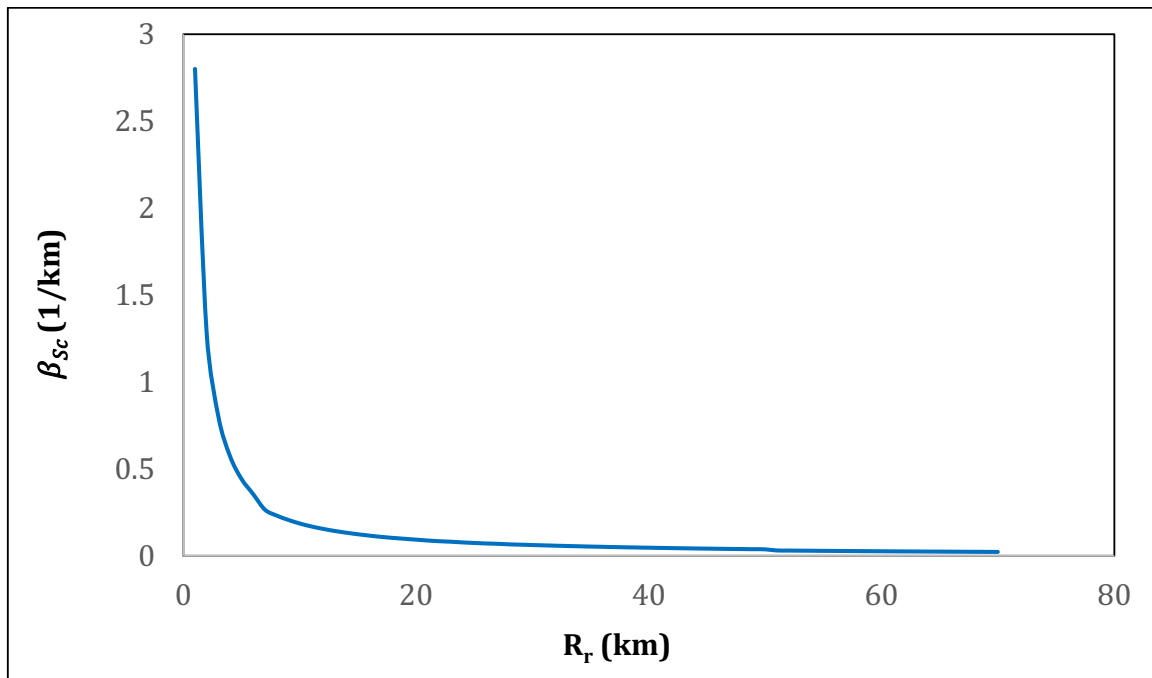
Figure 4.10 shows the scattering coefficient β_{Sc} $(1/km)$ as an exponential function of range R_r (km).
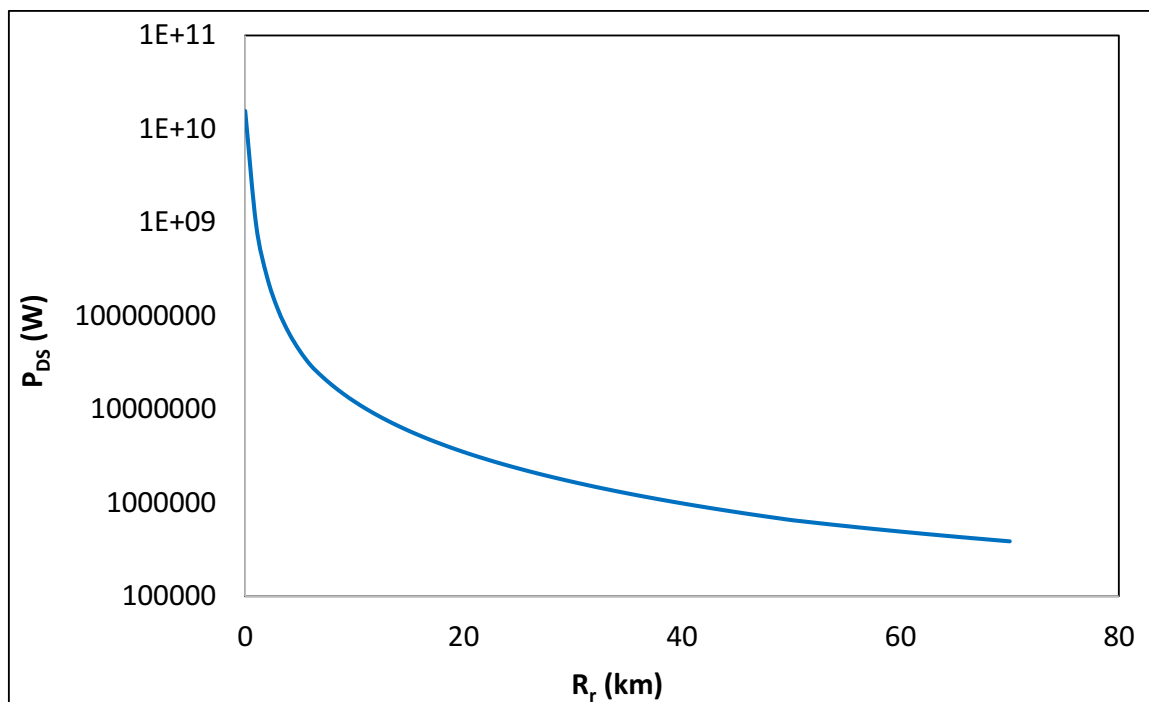

Figure 4.11 shows the effect of scattering coefficient on laser beam P_{DS} (W) as a function of range R_r (km).

From figure above, it can show the effect of the scattering coefficient which is significant in the first layer (0-11 km) because the all-weather change occurs in the first layer and this effect decreases with altitude.

The effect of the rainfall and snow on the laser beam was calculated according to equation (2.33-2.36) and it is shown in figure 4.12, we use the rate of rainfall and snow of Canada for November 2016 as an example for study [74].
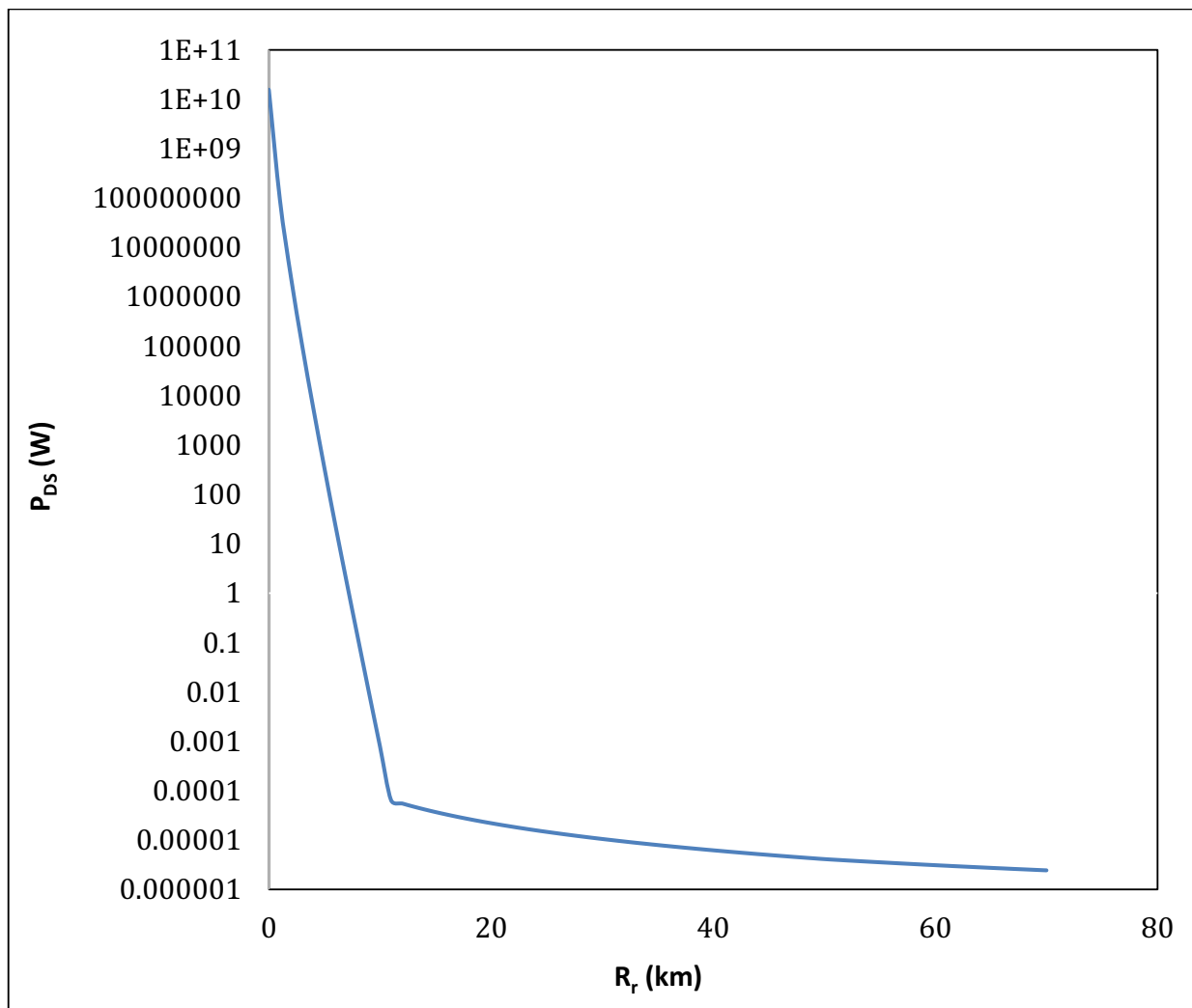

Figure 4.12 shows the effect of rainfall, snow and scattering on laser beam P_{DS} (W) as a function of range R_r (km).

The effect of rainfall and snowfall on the FELDS is very high, so most of the loss of FELDS power occurs in the first layer (see table 4.2). The atmospheric conditions should be observed before designing the weapon.

4.5   Atmospheric Turbulence

The value of atmospheric turbulence air refractive index (n), index refraction structure factor(C_n^2), fried parameter(r_0), Laser beam divergence(δ) and target distance move(D_{ta}) was calculated by using equation (2.37-2.39 and 3.4), Table 4.3 shows the changing of atmospheric turbulence parameters with altitude. In high altitudes, the refractive-index n close to 1 in order to change in the pressure and the slight temperature. The change in the refractive index (n) with pressure (P_A) and altitude (R_A) respectively shown in figures 4.13 and 4.14.

Table 4.3 shows the changing of atmospheric turbulence parameters with altitude.

R_A (km)	n	$C_n^2\left(m^{-\frac{2}{3}}\right)$	$r_0(m)$	$\delta\ (m)$	$D_{ta}(cm)$ Aircraft	$D_{ta}(cm)$ Missile
0	1.0002754	$6.5x10^{-12}$	0.008	0	0	0
5	1.0001652	$2.9x10^{-12}$	0.007	0.15	0.005	0.08
10	1.0000926	$1.3x10^{-12}$	0.010	0.30	0.011	0.17
15	1.0000431	$4.0x10^{-13}$	0.017	0.46	0.017	0.26
20	1.0000196	$8.2x10^{-14}$	0.040	0.61	0.023	0.35
25	1.0000089	$1.6x10^{-14}$	0.099	0.76	0.029	0.43
30	1.0000042	$3.3x10^{-15}$	0.242	0.91	0.035	0.52
35	1.0000019	$7.2x10^{-16}$	0.566	1.06	0.040	0.61

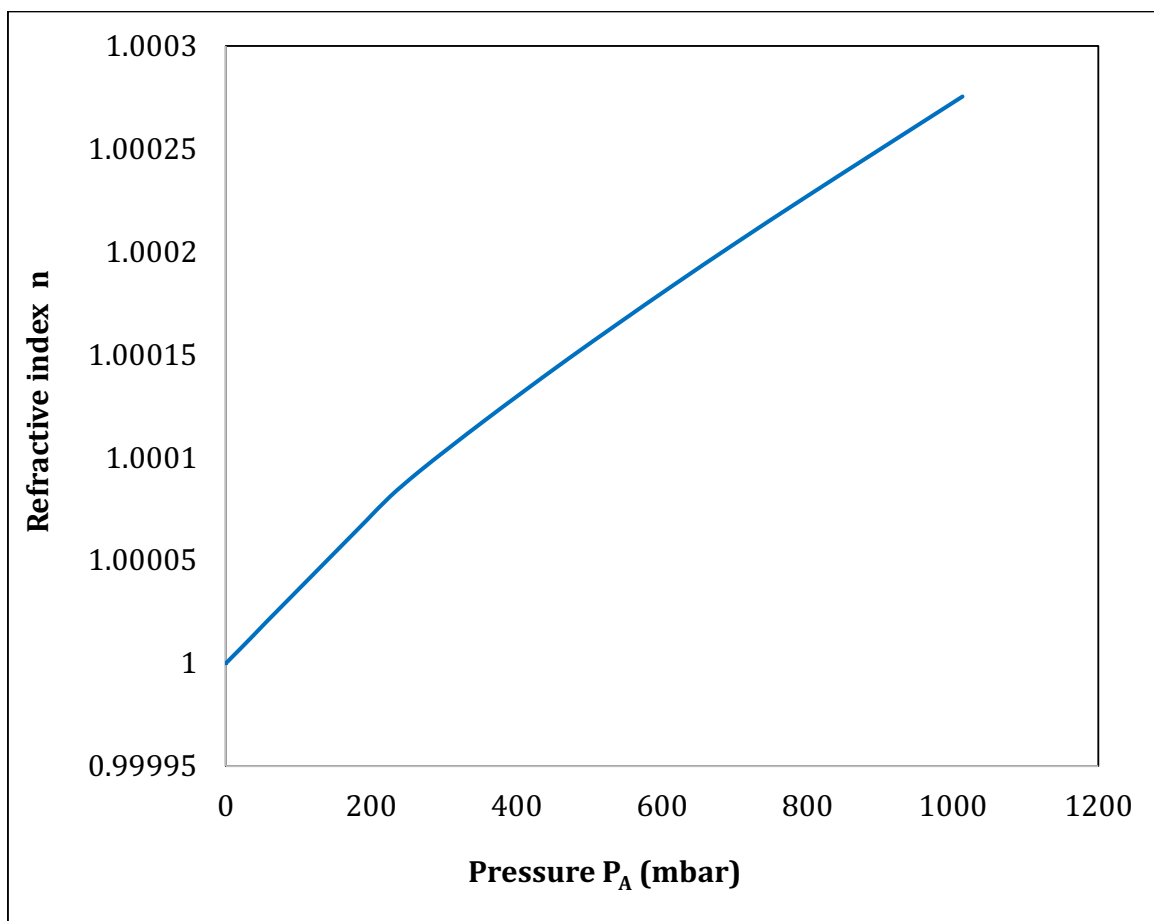| 40 | 1.0000010 | $1.4x10^{-16}$ | 1.43 | 1.22 | 0.046 | 0.70 |
45	1.0000005	$3.2x10^{-17}$	3.33	1.37	0.052	0.78
50	1.00000027	$1.0x10^{-17}$	6.39	1.52	0.058	0.87
55	1.00000015	$3.1x10^{-18}$	12.67	1.67	0.064	0.96
60	1.00000008	$1.0x10^{-18}$	24.09	1.83	0.070	1.05
65	1.000000035	$2.8x10^{-19}$	50.52	1.98	0.075	1.13
70	1.000000015	$6.4x10^{-20}$	119.03	2.13	0.081	1.22

Figure 4.13 shows the change in refractive index n with Pressure P_A (mbar).
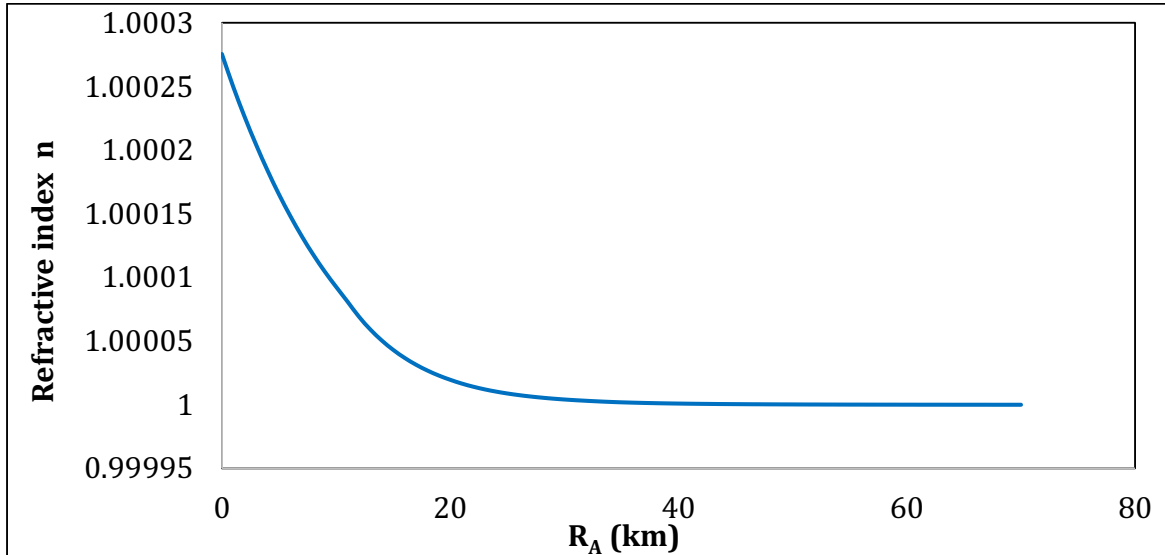
Figure 4.14 shows the change in refractive index n with altitude R_A (Km).

The refractive index structure constant (C_n^2) is used to determine the strength of atmospheric turbulence. It's inversely proportional with altitude according to equation (2.38), when (C_n^2) increases lead to increase in atmospheric turbulence. Figure 4.15 shows the change in the index of refraction structure parameter (C_n^2) in unit of (m $^{-2/3}$) with altitude (R_A).
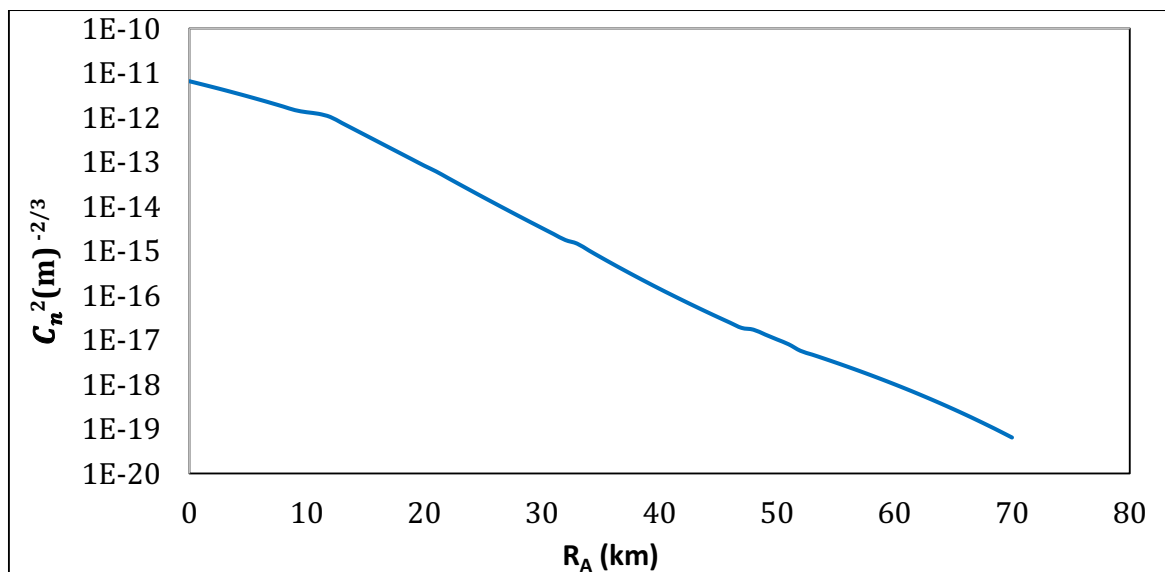

Figure 4.15 shows the change in the index of refraction structure parameter C_n^2 in unit of (m $^{-2/3}$) with altitude R_A.

The turbulence of refractive index structure constant (C_n^2) is very high in the first layer (10^{-12}), it will greatly attenuate the FELDS Power but this effect of C_n^2 decreases at altitude 70 km the($C_n^2 = 10^{-20}$).

According to Equation (2.39, 3.4), it was determined the laser beam divergence (δ) and Fried parameter (r_0) as a function with range (R_r). Figure 4.16 illustrates this relation, where r_0 defines as a circular diameter over which the laser beam maintains coherence. The lower value of r_0 implies stronger turbulence. Where the turbulence is very strong in the lower atmosphere, due to the significant temperature change in those layers according to equation (2.28). Based on the above, the upper atmosphere is ideal for laser weapons, due to low values of both turbulence and scattering.

The divergence of laser beam makes a problem to destroy the target, for solving this problem it can use the convex lens use to focus this beam on the target without divergence.
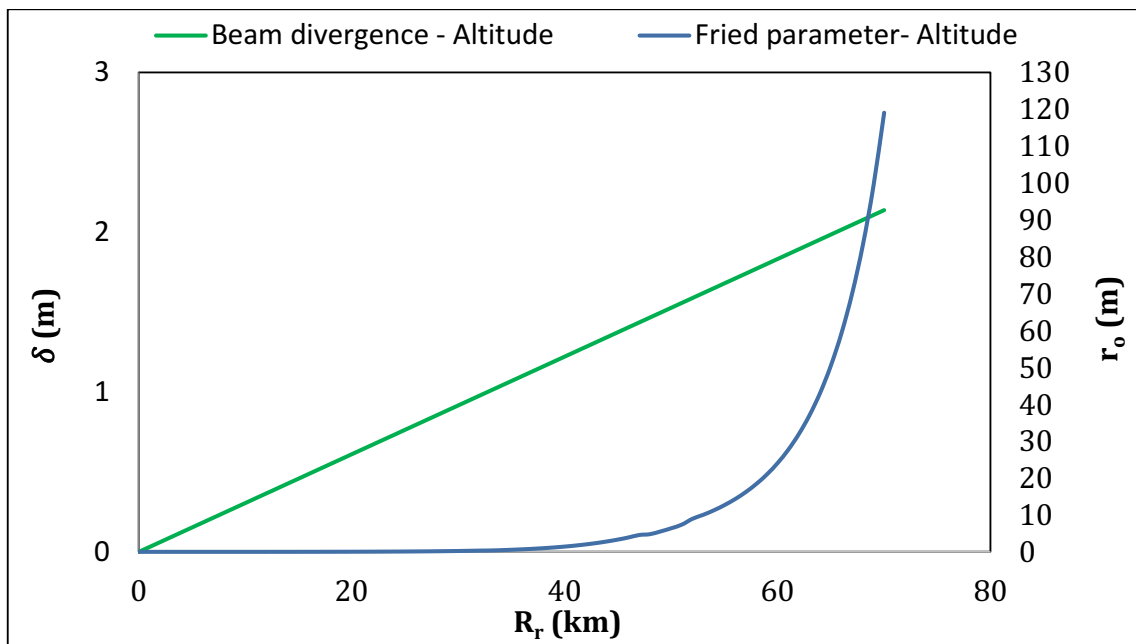

Figure 4.16 shows the laser beam divergence (δ) and Fried parameter r_0 as a function with rang R_r.

4.6   The Extra Distance of Target

For the aircraft and missile, the extra distance (D_{ta}) is calculated during the time period between the moments of launch of the laser beam from the FELDS to the moment falls on the target (based on equation (3.3)).

Figure 4.17 shows the extra distance for aircraft and missile, that means an increase in the time needed to deliver the power between the laser FELDS and the target, where (D_{ta}) depends on the speed of the target.

It is worth mentioning that the extra distance of the missile is larger than the aircraft, due to the speed of the missile is much greater than the speed of the aircraft.
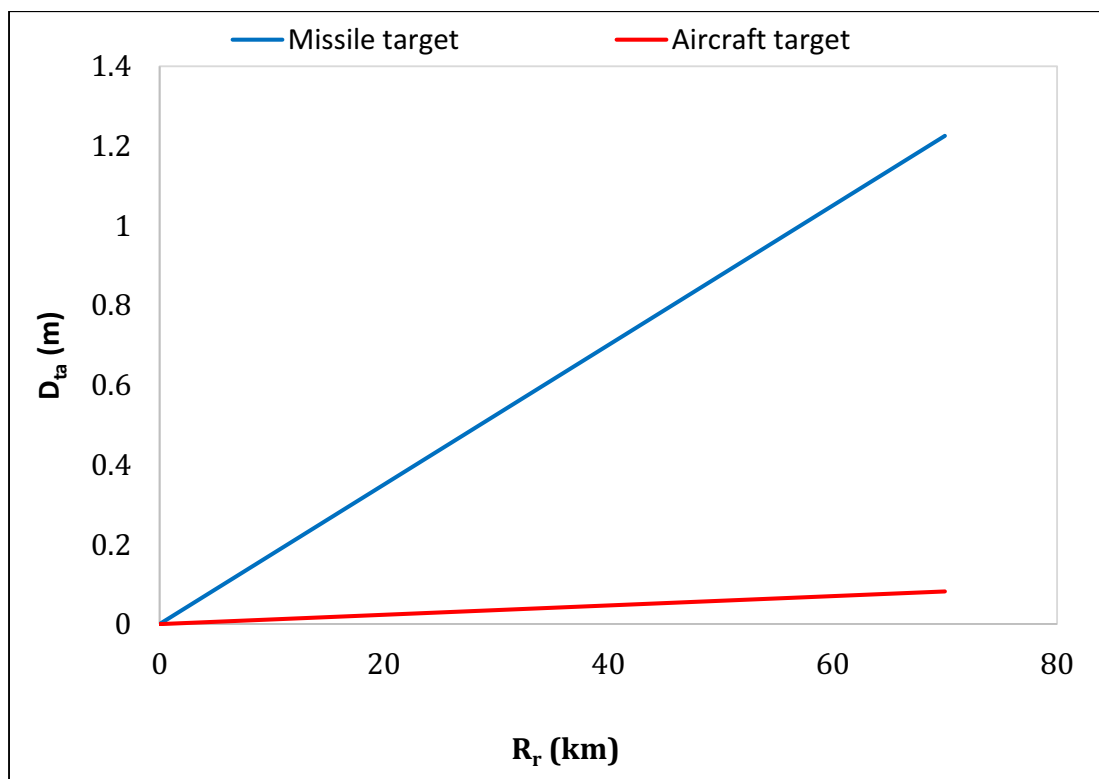

Figure 4.17 shows the extra distance for aircraft and missile.

4.7   The Power Needed to Destroy the Target

The actual power P_{actual} (kW) needed to destroy the target (Its external surfaces are made of steel or aluminum) as a function with altitude R_A (km). It was calculated according to equation (3.11, 3.12), Table 4.4 shows the actual power needed to destroy the target for steel and aluminum. Figure 4.18 shows the change in the power need as a result to the change of altitude R_A (km). The power needed to destroy the target varies depending on the altitude of the target from the sea level. This variation is due to the different temperatures of the different atmosphere layers, where the amount of power needed varies depending on the equation Eq. 3.11

Table 4.4 shows the actual power needed to destroy the target for steel and aluminum.

R (km)	P_{Tm} for Steel in (kW)	P_{actual} for Steel in (kW)	P_{Tm} for aluminum in (kW)	P_{actual} for aluminum in (kW)
0	38.30	382.98	22.03	220.26
5	38.37	383.70	22.08	220.76
10	38.44	384.42	22.13	221.26
15	38.46	384.57	22.14	221.36
20	38.46	384.57	22.14	221.36
25	38.45	384.46	22.13	221.28
30	38.43	384.35	22.12	221.20
35	38.41	384.12	22.10	221.04
40	38.38	383.80	22.08	220.83
45	38.35	383.49	22.06	220.61
50	38.34	383.37	22.05	220.53

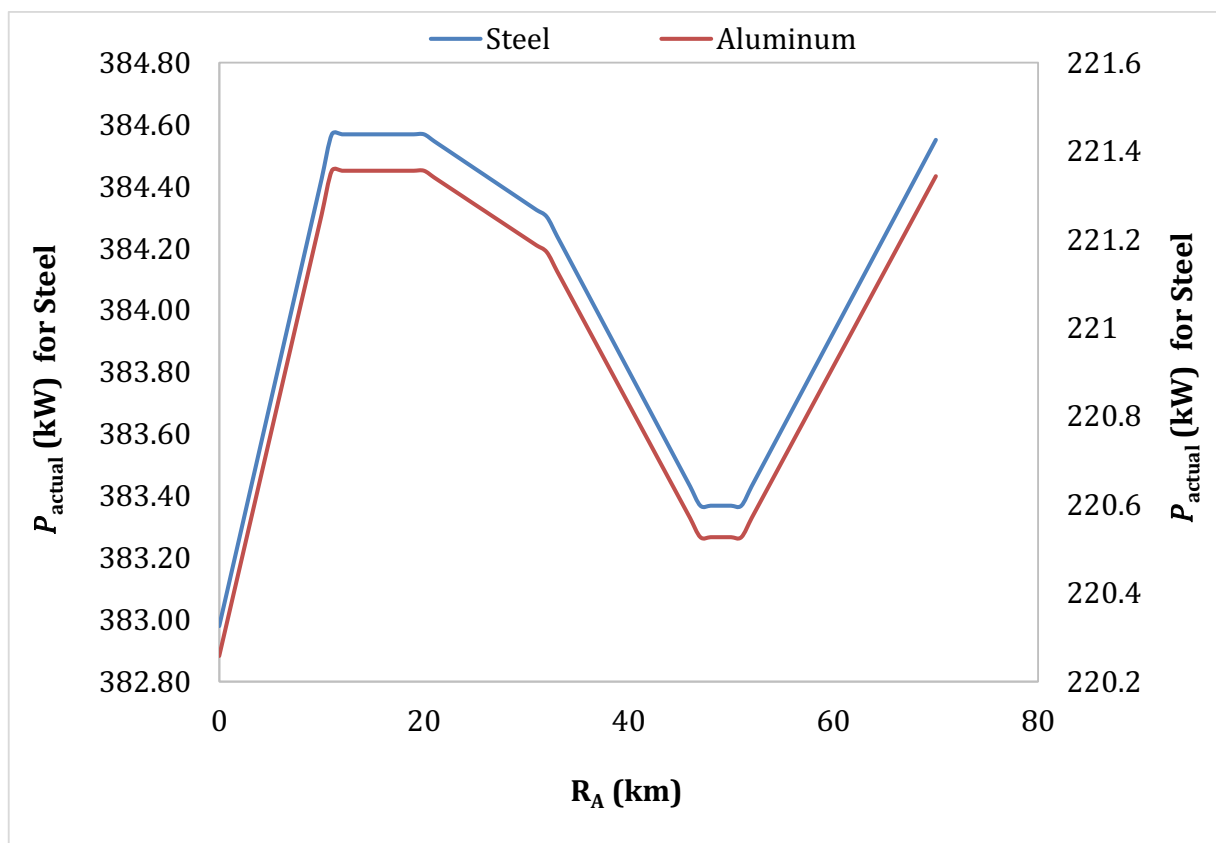| 55	38.36	383.62	22.07	220.70
60	38.39	383.93	22.09	220.91
65	38.42	384.24	22.11	221.13
70	38.46	384.55	22.13	221.34

Figure 4.18 shows the change in the actual power need to destroy the target (steel or aluminum) P_{actual}(kw) with altitude R_A (km).

Chapter Five Conclusions and Suggestions for Future Work

Chapter Five

Conclusions and Suggestions for Future Work

5.1 Conclusions

From previous results of free electron laser FIELDS, it can be concluded the following:

1. The atmosphere affects significantly on the effectiveness of free electron laser FELDS, which is produced from temperature fluctuations, construction of the gas and dust atoms.

2. The weather changes occur in the troposphere layer (0-11 km), so that the turbulence effect significantly on the laser beam of FELDS, While their effect decreases as we move away from the troposphere, because the mass of the atmosphere is concentrated in the troposphere.

3. The effect of rainfall and snowfall on the beam of FELDS is significantly appears in the first layer of the atmosphere (0-1 Km).

4. The divergence of laser beam makes a problem to destroy the target, for solving this problem we can use the convex lens which is used to focus this beam on the target without divergence.

5. In perfect weather case (without rainfall and snowfall) this design of FELDS can be effective on the target (destroy the target at altitude 70 Km) with output power about (388000 KW).

5.2 Suggestions for Future Work

1- Designing a free electron laser weapon with a wavelength within the X-ray region produces high destructive power.

2- Increase the effectiveness and energy of FELDS destruction by developing and enlarging laser resonator mirrors

3- Try to increase the range of the FELDS for more than 70km by increasing the length of undulator.

4- Changing the initial shape of the undulator with new dimensions in the form of vertical rows to reduce the size of the free electron laser.

Appendix

Free electron laser defense system (FELDS) program

In this work, a new free electron laser defense system (FELDS) is designed and details of its steps are shown in Figure 1
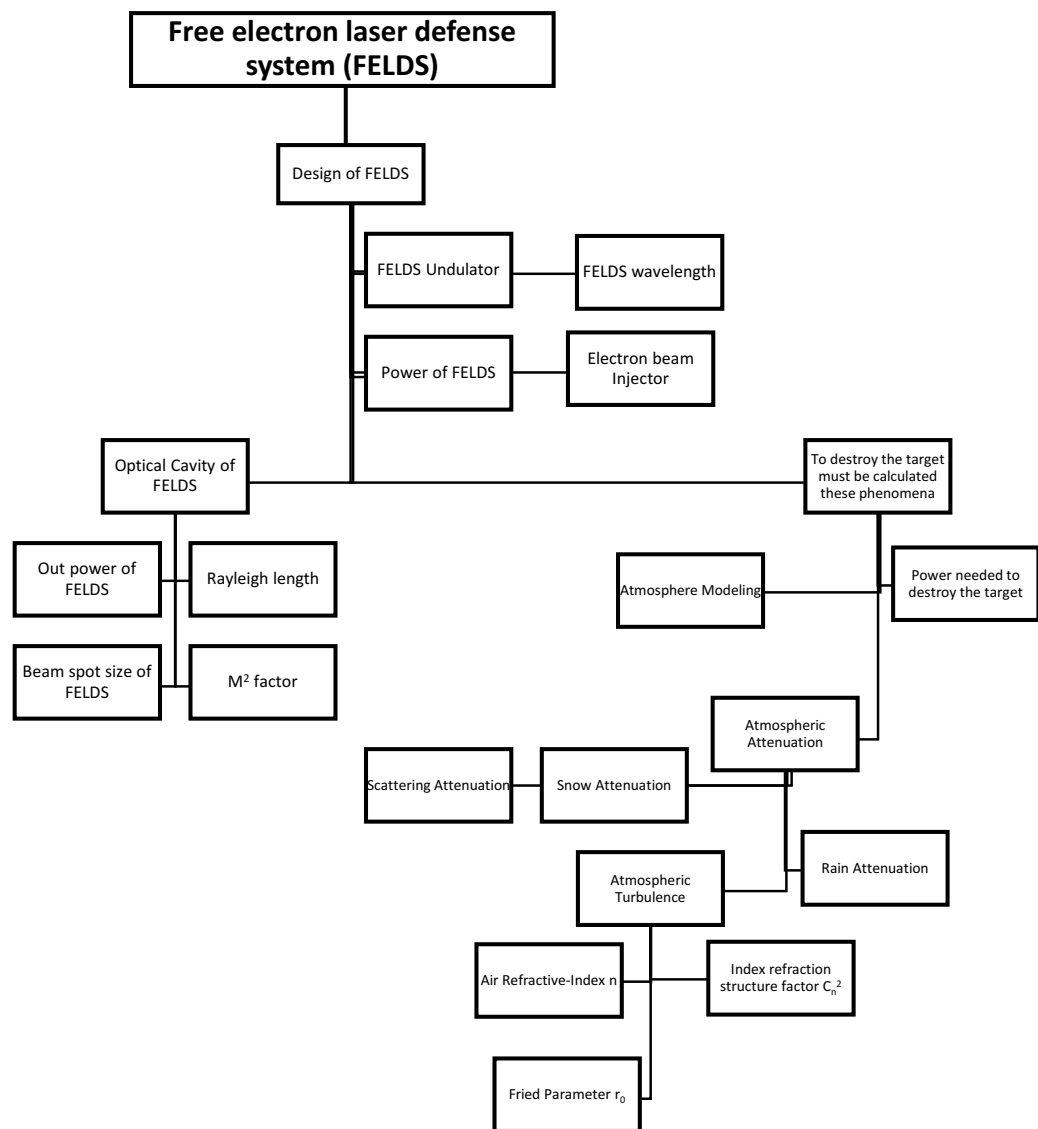
Fig. 1: Flowchart of Free Electron Laser Defense System (FELDS).

Also, it has been established special program using Visual Basic 2010 programming language, which contains many parameters as shown in Figure2.

Fig. 2: Shows the design of FELDS program.

Contents of the program

The program 'Free electron laser defenses system (FELDS) 'consists of three units:

- *Input unit*
- *Account unit*
- *Output unit*

These units contain many functions and parameters, which are based on a set of basic laws used to get the results described in chapter four.

Input unit

- *Electron beam energy E_{beam}*
- *Wavelength of wiggler λ_m*
- *Undulator gap g_w*
- *Undulator length Z_w*
- *Initial beam size of the electron beam σ*
- Beam current *of the electron beam I_{beam}*
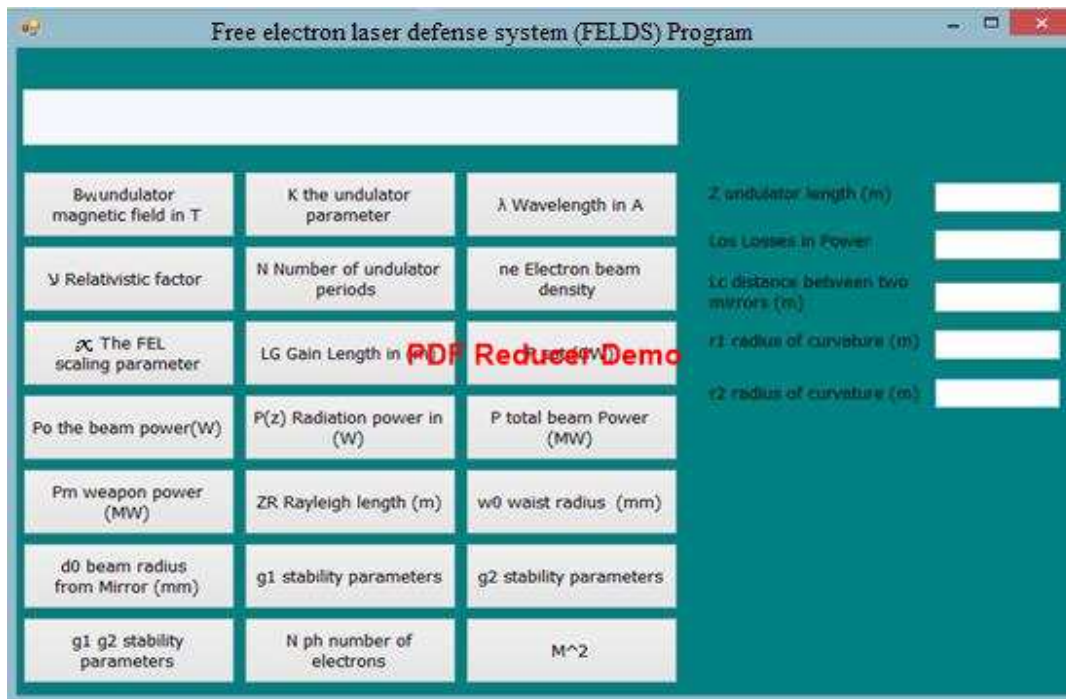- Classical radius of the electron r_e
- *Light speed c*
- *Electron Charge e*
- *Electron mass m_e*
- *Reflection of mirrors R_1, R_2*
- *The radius of curvature r_1, r_2*
- *Distance between two mirrors L_c*

Account unit

- *laser wavelength $\lambda = \lambda_m \left(\frac{1}{2\gamma^2} + \frac{K^2}{4\gamma^2} \right)$*

- Relativistic Lorentz-factor $\gamma = E_{beam}/m_e c^2$

- *Wiggler parameter $K = 0.934\, B_w\, \lambda_m$*

- *Number of undulator periods $N_u = Z_w/\lambda_m$*

- *Scaling parameter of FEL $\chi = \sqrt[3]{\left(\frac{a_w\, w_p}{4\gamma\, w_c} F(k) \right)^2}$*

- The gain-length $L_G = \frac{\lambda_m}{4\,\pi\,\sqrt{3}\,\chi}$

- *Electron beam density $n_e = \frac{I_{beam}}{2\pi e c \sigma^2}$*

- Magnetic field $B_w = 4.22 \exp\left[-\frac{g_w}{\lambda_m}\left(5.08 + 1.54\, \frac{g_w}{\lambda_m} \right) \right]$

- *Resonator stability $g_1 = (1 - \frac{L_c}{r_1}),\ g_2 = (1 - \frac{L_c}{r_2})$*

- *Power FELDS $P_m = P_z\, R_1\, R_2\, e^{2L_c\,(G - \forall)}$*

- Rayleigh length $Z_R = \sqrt{\frac{g_1 g_2 (1 - g_1 g_2) L_c^2}{(g_1 + g_2 - 2 g_1 g_2)^2}}$

- Beam spot size $d_{mirror} = d_0 \sqrt{[1 + \left(\frac{L_c}{2\,Z_R}\right)^2]}$

- Quality-factor $M^2 = \frac{\pi\,\omega_0^2}{Z_R\,\lambda}$.

🞣 *Output unit*

    A white screen to display the results

    Below is part of the language of the program, in which the simulation was done and the results obtained.

Private Sub Button4_Click(ByVal sender As System.Object, ByVal e As System.EventArgs) Handles Button4.Click

    TextBox1.Text = (((Val(TextBox4.Text) * 10 ^ 8) / (2 * ((1.957 * 10 ^ 3 * Val(TextBox3.Text)) ^ 2))) * (1 + (((0.934 * Val(TextBox5.Text) * Val(TextBox4.Text)) ^ 2) / 2)))

    x = Val(TextBox1.Text)

    ArithmeticProcess = " ((Val(TextBox4.text)*10^8)/(2 * ((1.957 * 10 ^ 3 * Val(TextBox3.Text)) ^ 2)))*(1 + (((0.934 * Val(TextBox5.Text) * Val(TextBox4.Text)) ^ 2) / 2)) "

    End Sub

TextBox1.Text = ((((0.934 * Val(TextBox5.Text) * Val(TextBox4.Text) * 10 ^ -2) * (((4 * 3.14 * 2.817 * 10 ^ -15 * 9 * 10 ^ 16 * ((Val(TextBox9.Text) * 10 ^ 3) / (2 * 3.14 * 1.6 * 10 ^ -19 * 3 * 10 ^ 8 * (Val(TextBox7.Text) * 10 ^ -6 * Val(TextBox15.Text) * 10 ^ -6)))) / (Val(TextBox3.Text) / (0.511 * 10 ^ -3))) ^

0.5)) / (4 * (Val(TextBox3.Text) / (0.511 * 10 ^ -3)) * ((2 * 3.14 * 3 * 10 ^ 8) / (Val(TextBox4.Text) * 10 ^ -2)))) ^ (2 / 3))

 x = Val(TextBox1.Text)

 ArithmeticProcess = " (((((0.934 * Val(TextBox5.Text) * Val(TextBox4.Text) * 10 ^ -2) * (((4 * 3.14 * 2.817 * 10 ^ -15 * 9 * 10 ^ 16 * ((Val(TextBox9.Text) * 10 ^ 3) / (2 * 3.14 * 1.6 * 10 ^ -19 * 3 * 10 ^ 8 * (Val(TextBox7.Text) * 10 ^ -6 * Val(TextBox15.Text) * 10 ^ -6)))) / (Val(TextBox3.Text) / (0.511*10^-3))) ^ 0.5)) / (4 * (Val(TextBox3.Text) / (0.511*10^-3)) * ((2 * 3.14 * 3 * 10 ^ 8) / (Val(TextBox4.Text) * 10 ^ -2)))) ^ (2 / 3)) "

 End Sub

References

[1] J. B. Murphy and C. Pellegrini, "Introduction to the physics of the free electron laser," *Front. Part. Beams*, pp. 163–219, 1988.

[2] Y. Socol, "High-power free-electron lasers–technology and future applications," *Opt. Laser Technol.*, vol. 46, pp. 111–126, 2013.

[3] S. Krishnagopal and V. Kumar, "Free-electron lasers," *Radiat. Phys. Chem.*, vol. 70, no. 4, pp. 559–569, 2004.

[4] D. D. Dlott and M. D. Fayer, "Applications of infrared free-electron lasers: basic research on the dynamics of molecular systems," *IEEE J. Quantum Electron.*, vol. 27, no. 12, pp. 2697–2713, 1991.

[5] T. I. Smith, "The source issue in infrared microspectroscopy," *Nucl. Instrum. Methods Phys. Res. Sect. Accel. Spectrometers Detect. Assoc. Equip.*, vol. 483, no. 1, pp. 565–570, 2002.

[6] B. M. Deveci, "Directed-Energy Weapons: Invisible and Invincible," MSc thesis, Monterey, California. Naval Postgraduate School, USA, 2007.

[7] L. D. Welch and R. J. Hermann, "*Defense Science Board Task Force on Directed Energy Weapons* ", Defense Science Board Washington, 2007.

[8] R. O'Rourke, "Navy shipboard lasers for surface, air, and missile defense: Background and issues for Congress," 2013.

[9] L. D. Welch and D. C. Latham, "Defense science board task force on high energy laser weapon systems applications," Defense Science Board Washington, 2001.

[10] J. Stupl and G. Neuneck, "Assessment of long range laser weapon engagements: The case of the airborne laser," *Sci. Glob. Secur.*, vol. 18, no. 1, pp. 1–60, 2010.

[11] M. Achour, "Free-space optics wavelength selection: 10 μm versus shorter wavelengths [invited]," *J. Opt. Netw.*, vol. 2, no. 6, pp. 127–143, 2003.

[12] Z. Ghassemlooy, M. Awan, E. Leitgeb, and W. O. Popoola, "Atmospheric channel effects on terrestrial free space optical communication links," 2009.

[13] J. M. Madey, "Stimulated emission of bremsstrahlung in a periodic magnetic field," *J. Appl. Phys.*, vol. 42, no. 5, pp. 1906–1913, 1971.

[14] L. R. Elias, W. M. Fairbank, J. M. Madey, H. A. Schwettman, and T. I. Smith, "Observation of stimulated emission of radiation by relativistic electrons in a spatially periodic transverse magnetic field," *Phys. Rev. Lett.*, vol. 36, no. 13, p. 717, 1976.

[15] R. Ruquist, "Variable atmosphere effects on high energy laser propagation," *J. Phys. Colloq.*, vol. 41, no. C9, pp. C9–121, 1980.

[16] R. Bonifacio, C. Pellegrini, and L. M. Narducci, "Collective instabilities and high-gain regime in a free electron laser," *Opt. Commun.*, vol. 50, no. 6, pp. 373–378, 1984.

[17] K. S. Shaik, "Atmospheric propagation effects relevant to optical communications," *NASA technical reports server*,1988.

[18] E. J. Anderson, "Total ship integration of a Free Electron Laser (FEL)," MSc thesis, Monterey, California. Naval Postgraduate School, USA, 1996.

[19] S. Zhengfang, "Atmospheric attenuation of common applied lasers," *National air intelligence center*, China, 1997.

[20] Ng. Ivan, "A free electron laser weapon for sea archer," MSc thesis, Monterey, California. Naval Postgraduate School, USA, 2001.

[21] I. I. Kim, B. McArthur, and E. J. Korevaar, "Comparison of laser beam propagation at 785 nm and 1550 nm in fog and haze for optical wireless communications," in *Information Technologies 2000*, 2001, pp. 26–37.

[22] G. Dattoli and P. L. Ottaviani, "Semi-analytical models of free electron laser saturation," *Opt. Commun.*, vol. 204, no. 1, pp. 283–297, 2002.

[23] X. Yaoheng and F. Hesheng, "Modification of laser ranging equation," in *Proceedings of the 13th international workshop on laser ranging, Washington, DC*, 2002.

[24] S. Krinsky, G. A. Smith, and T. Russo, "The Physics and Properties of Free-Electron Lasers," in *AIP Conference Proceedings*, USA, 2002, vol. 648, pp. 23–43.

[25] C. Pellegrini, "X-ray free-electron lasers and ultrafast science at the atomic and molecular scale," in *Proc. European Particle Accelerator Conference, Edinburgh*, 2006, pp. 3636–3639.

[26] D. Cowan, "Effects of atmospheric turbulence on the propagation of flattened Gaussian optical beams," University of Central Florida Orlando, Florida, 2006.

[27] Z. Huang and K.-J. Kim, "Review of x-ray free-electron laser theory," *Phys. Rev. Spec. Top.-Accel. Beams*, vol. 10, no. 3, p. 34801, 2007.

[28] M. Beshr and M. H. Aly, "Outdoor Wireless Optical Communication System Attenuation at Different Weather Conditions," *Arab Acad. Sci.*, pp. 194–199, 2008.

[29] M. Hussein, "Scintillation Effect on Satellite Communications within Standard Atmosphere," *Anbar J. Eng. Sci.*, vol. 2, no. 2, pp. 17–27, 2009.

[30]   O. Wilfert and others, "Laser beam attenuation determined by the method of available optical power in turbulent atmosphere," *J. Telecommun. Inf. Technol.*, pp. 53–57, 2009.

[31]   O. Wilfert and L. Dordova, "Calculation and Comparison of Turbulence Attenuation by Different Methods," *Radioengineering*, 2010.

[32]   M. Abd Ali, "Free Space Lasers Propagation at Different Weather Conditions," *Al- Mustansiriyah J Sci*, vol. 23, no. 2, pp. 81–90, 2012.

[33]   A. Alkholidi and K. Altowij, *Effect of clear atmospheric turbulence on quality of free space optical communications in Western Asia*. INTECH Open Access Publisher, 2012.

[34]   M. Bakr *et al.*, "Design and Numerical Simulation of THZ-FEL Amplifier in Kyoto University," in *THz and Long Wavelength FELs*, Nara, Japan, 2012, vol. WEPD65, pp. 519–522.

[35]   M. Ali and M. Mohammed, "Effect of atmospheric attenuation on laser communications for visible and infrared wavelengths," *J Al-Nahrain Univ.*, vol. 16, no. 3, pp. 133–140, 2013.

[36]   P. Pan, "Study on Turbulence Effects for Beam Propagation in Turbulent Atmosphere," *Opt. Photonics J.*, vol. 3, no. 2, p. 143, 2013.

[37]   M. Shanshoul, M. Albek, and S. Kelesh, "Study of Atmosphere ic Penetration Factors for Near Infrared Laser Beam (0.980 μm) Performing as a Carrier Data in Free Space Rainy Atmospheric Conditions," *Rafidain J. Sci.*, vol. 24, no. 3, pp. 86–101, 2013.

[38]   A. R. Jabbar, F. A.-Z. Morad, and I. A. Murdas, "Performance Evaluation of High Speed Optical Wireless Communication System Based on Atmospheric Turbulence (Fog Effect)," *Int. J. Sci. Res. IJSR*, vol. 10, no. 5, pp. 628–632, 2013.

[39] M. A. A. Ali, "Free Space Optical Wireless Communications under Turbulence Channel Effect," *IOSR J. Electron. Commun. Eng.*, vol. 9, no. 3, pp. 1–8, 2014.

[40] L. Song, Y. Ding, and Q. Liu, "BER Characteristics Analysis of Atmosphere Laser Propagation in A Variety Of Weather Factors," *Int. J. Innov. Comput. Inf. Control*, vol. 10, no. 4, pp. 1447–1455, 2014.

[41] A. N. Z. Rashed and M. S. Tabbour, "Free Space Optics and Submarine Laser Communication Systems for Egyptian Climate Weather in the Presence of Atmospheric Turbulence," *Int. J. Res. Electron. Commun. Technol.*, vol. 1, no. 1, pp. 34–40, 2014.

[42] M. Firoozmand and M. Naser-Moghadasi, "Modeling and Simulation of Fading Due of Atmospheric Turbulence by Chi-Squared and Exponential pdf for a FSO Link," *NNGT IntJNetworking Comput.*, vol. 2, pp. 1–9, 2015.

[43] S. Di Mitri, "On the Importance of Electron Beam Brightness in High Gain Free Electron Lasers," in *Photonics*, 2015, vol. 2, pp. 317–341.

[44] S. A.Kadhim, A. H. Dagher, J. A. Kalati, and N. A. Al-Jaber, "Light Attenuation Measurements at 650 and 850nm Wavelengths in Dense Fog and Smoke for FSO Applications," *Int. J. Res. Electron. Commun. Technol.*, vol. 5, no. 3, pp. 3439–3444, 2016.

[45] R. Bonifacio, H. Fares, M. Ferrario, B. W. McNeil, and G. R. Robb, "Design of sub-Angstrom compact free-electron laser source," *Opt. Commun.*, vol. 382, pp. 58–63, 2017.

[46] T. Liu, T. Zhang, D. Wang, and Z. Huang, "Compact beam transport system for free-electron lasers driven by a laser plasma accelerator," *Phys. Rev. Accel. Beams*, vol. 20, no. 2, pp. 1–10, 2017.

[47]   E. J. Jaeschke, S. Khan, J. R. Schneider, and J. Hastings, *Synchrotron Light Sources and Free-Electron Lasers: Accelerator Physics, Instrumentation and Science Applications*. Switzerland: Springer Reference, 2016.

[48]   V. Kumar and K.-J. Kim, "Analysis of Smith-Purcell free-electron lasers," *Phys. Rev. E*, vol. 73, no. 2, p. 26501, 2006.

[49]   A. Yahaghi, A. Fallahi, and F. Kärtner, "Free Electron Laser Simulation Tool Based on FDTD/PIC in the Lorentz Boosted Frame," in *7th International Particle Accelerator Conference (IPAC'16), Busan, Korea, May 8-13, 2016*, 2016, pp. 3061–3063.

[50]   E. Di Palma, E. Sabia, G. Dattoli, S. Licciardi, and I. Spassovsky, "Cyclotron auto resonance maser and free electron laser devices: a unified point of view," *J. Plasma Phys.*, vol. 83, no. 1, pp. 1–15, 2017.

[51]   J. van Tilborg, S. K. Barber, F. Isono, C. B. Schroeder, E. Esarey, and W. P. Leemans, "Free-electron lasers driven by laser plasma accelerators," in *AIP Conference Proceedings*, 2017, vol. 1812, pp. 1–7.

[52]   P. Baxevanis, Z. Huang, R. Ruth, and C. B. Schroeder, "Eigenmode analysis of a high-gain free-electron laser based on a transverse gradient undulator," *Phys. Rev. Spec. Top.-Accel. Beams*, vol. 18, no. 1, pp. 1–10, 2015.

[53]   J. Pyrhonen, T. Jokinen, and V. Hrabovcova, *Design of rotating electrical machines*. John Wiley & Sons, 2009.

[54]   T. Liu, Z. Huang, B. Liu, J. Liu, D. Wang, and T. Zhang, "Beam Transport Line of the LPA-FEL Facility Based on Transverse Gradient Undulator," in *7th International Particle Accelerator Conference (IPAC'16), Busan, Korea, May 8-13, 2016*, pp. 3287–3290.

[55]   R. P. Mansfield, "High energy solid state and free electron laser systems in tactical aviation," MSc thesis, Monterey, California.Naval Postgraduate School, USA, 2005.

[56]   H. D. Yildiz, "Infrared Free Electron Laser, Resonator Parameters Optimization with Genesis, Opc and Glad Codes," *Math. Comput. Appl.*, vol. 16, no. 2, pp. 659–668, 2011.

[57]   E. Kochkina, "Stigmatic and Astigmatic Gaussian Beams in Fundamental Mode: Impact of Beam Model Choice on Interferometric Pathlength Signal Estimates" Technische Informationsbibliothek und Universitätsbibliothek Hannover (TIB) Hannover, 2013.

[58]   T. Plath, C. Lechner, S. Ackermann, and J. Bödewadt, "Influence of Seed Laser wave front Imperfections On HGHG Seeding Performance," *Seeded FELs*, pp. 643–645, 2015.

[59]   M. B. Alsous, M. Almezel, and M. Alnezami, "Monte Carlo Least-Squares Fitting of the Beam Propagation Factor M2," *Acta Phys. Pol. A*, vol. 124, no. 4, pp. 673–676, 2013.

[60]   F. Marc, H. G. de Chatellus, and J.-P. Pique, "Effects of laser beam propagation and saturation on the spatial shape of sodium laser guide stars," *Opt. Express*, vol. 17, no. 7, pp. 4920–4931, 2009.

[61]   M. Cavcar "The international standard atmosphere (isa)" *Anadolu Univ. Turk.*, vol. 30, 2000.

[62]   T. S. McKechnie, *''General theory of light propagation and imaging through the atmosphere''*, vol. 196. USA: Springer, 2016.

[63]   B. M. Smirnov, *''Microphysics of Atmospheric Phenomena'' Springer*, Russia, 2016.

[64] R. A. Minzner, *The 1976 Standard Atmosphere Above 86-km Altitude*, 1976th ed. NATIONAL AERONAUTICS AND SPACE ADMINISTRATION.

[65] M. S. Islam, A. B. Mohammad, and S. A. Al-Gailani, "Characteristics of free space optics communication link in an unusual haze," *Indian J. Pure Appl. Phys.*, vol. 54, pp. 46–50, 2016.

[66] S. Pradhan, R. K. Panigrahy, A. Kumar, A. K. Prajapati, and A. K. Mallick, "Performance Analysis and System Design of the Performance Characterization of Data Transmission on Free Space Optics (FSO) by using Optic System 14.0," *Int. J. Eng. Technol.*, vol. 3, no. 5, pp. 63–67, 2016.

[67] R. Reghunadh and L. G.B, "Efficiency Comparison of Diversity Techniques in FSO links for Fading mitigation using EDFA and APD," *Int. J. Innov. Res. Comput. Commun. Eng.*, vol. 5, no. 3, pp. 4150–4157, 2017.

[68] M. M. Shumani, M. F. L. Abdullah, and A. Z. Suriza, "The Effect of Haze Attenuation on Free Space Optics Communication (FSO) at Two Wavelengths under Malaysia Weather," in *Computer and Communication Engineering (ICCCE), 2016 International Conference on*, 2016, pp. 459–464.

[69] P. Kumari and R. Thakur, "Review Paper: Hybrid Amplifiers in FSO System," *Int. J. Comput. Tech.*, vol. 3, no. 2, pp. 115–123, 2016.

[70] W. J. Ng, "Design and analysis of megawatt class Free Electron Laser weapons," MSc thesis, Monterey, California: Naval Postgraduate School, USA, 2015.

[71] A. L. Puryear, "Optical communication through the turbulent atmosphere with transmitter and receiver diversity, wavefront control, and coherent detection," Ph.D. thesis, Massachusetts Institute of Technology, 2011.

[72] S. M. A. Shah, M. S. A. Latiff, B. S. Chowdhry, and T. Riaz, "Investigation of Single Beam Near-Infrared Free Space Optical Communication Under Different Weather Anomalies," *ARPN J. Eng. Appl. Sci.*, vol. 11, no. 9, pp. 5732–5738, 2016.

[73] M. F. Talib, A. K. Rahman, M. S. Anuar, C. B. M. Rashidi, and S. A. Aljunid, "Investigation on Heavy Precipitation Effects over FSO Link," in *MATEC Web of Conferences*, vol. 97, p. 1113, 2017.

[74] P. W. N. Inc, "Statistics," *The Weather Network*. [Online]. Available: http://www.theweathernetwork.com/forecasts/statistics/precipitation/ cl6158350/caon0696/imperial. [Accessed: 26-Jun-2017].

الخلاصة

في هـذا العمـل، تـم تصـميم نمـوذج جديـد لمنظومـة دفـاع ليـزر الالكتـرون الحـر FELDS في نطـاق الأشـعة تحت الحمـراء وبطاقـة عاليـة لتدمير أي هدف (الصـاروخ او الطائرات) وبمدى 70 كم . ان تصميم أي نظام دفاع يتطلب معرفة خصـائص الهدف الذي سيتم تدميره ومـدى الهدف وحركتـه سواء كـان متجهـا نحـو منظومـة الدفـاع او مبتعدا. ان تصميم ليزر الإلكترون الحر يتضمن أربعة مكونـات أساسية هي قاذفة الإلكترونات ومعجل الإلكترونات والمجال المغناطيسي الدوري والمرنان البصري.

من أجل عمل محاكاة لنظام الدفاع، وتحديد متغيرات هذا النظام، فقد تم إنشاء برنامج خاص باستخدام لغة البرمجة فجوال بيسك 2010، يحتوي على العديد من المعلومـات لحسـاب وتحليل تأثير الغلاف الجوي (مثل الامتصاص والتشتت والضباب والمطر ومعامل الانعكاس ومعامل الانكسار وانفراج الحزمة) على شعاع الليزرالناتج من FELDS المـار عبر طبقات الغلاف الجوي المختلفة.

جمهورية العراق

وزارة التعليم العالي والبحث العلمي

جامعة بغـداد

كلية التربية للعلوم الصرفة ابن الهيثم

قسم الفيزياء

حساب وتحليل بعض التأثيرات الجوية على حزمة ليزر الالكترون الحر

رسالة مقدمة الى

مجلس كلية التربية للعلوم الصرفة ابن الهيثم/جامعة بغداد

كجزء من متطلبات نيل درجة ماجستير علوم في الفيزياء

من قبـــل

رشيد لطيف جواد جاسم

(بكالوريوس 2014)

بأشراف

أ.م. د. ثائر عبد الكريم خليل العايش

1438هـ   **2017 م**